



Inês Tadeu dos Anjos Simões

1º Ciclo de Bioquímica

**Functional and therapeutical implications
of ligand recognition by the scavenger-like
lymphocyte receptors CD5 and CD6**

Dissertação para obtenção do Grau de Mestre em
Genética Molecular e Biomedicina

Orientador: Francisco Lozano, Prof.Doutor, CEK
Co-orientador: Vanesa Martinez, Doutora, CEK
Co-orientador: Ana Madalena Ludovice, Prof.Doutora, FCT/UNL

Júri:

Presidente: Prof. Doutor José Paulo Sampaio
Arguente: Prof. Doutora Paula Alexandra Videira
Vogal: Doutora Vanesa Gabriela Martinez



FACULDADE DE
CIÊNCIAS E TECNOLOGIA
UNIVERSIDADE NOVA DE LISBOA

Novembro, 2011

Functional and therapeutical implications of ligand recognition by the scavenger-like lymphocyte receptors CD5 and CD6

Copyright Inês Tadeu dos Anjos Simões, FCT/UNL, UNL

A Faculdade de Ciências e Tecnologia e a Universidade Nova de Lisboa têm o direito, perpétuo e sem limites geográficos, de arquivar e publicar esta dissertação através de exemplares impressos reproduzidos em papel ou de forma digital, ou por qualquer outro meio conhecido ou que venha a ser inventado, e de a divulgar através de repositórios científicos e de admitir a sua cópia e distribuição com objectivos educacionais ou de investigação, não comerciais, desde que seja dado crédito ao autor e editor.

Acknowledgments

My utmost gratitude goes to my thesis advisor, Dr. Francisco Lozano Soto, for allowing me to join his team despite the paperwork that was necessary. Thank you for the opportunity to learn from you and trust in me!

It is a pleasure to thank the Immunoreceptors of the Innate and Adaptive System group, or as we say Paco's, for their hospitality. I am indebted to you, who made my stay in Barcelona a very pleasant one, scientifically and personally. Working in the lab was always a joy! Thank you to teach me how to be a scavenger!

I wouldn't be performing this work without two special persons who I had the privilege to work with. Rafael Fenutría, thank you for the hours spent in the biotherium and cytometer and all you have teach me. Vanesa Martinez, thank you for your continual encouragement and support. This thesis would not have been possible without your guidance, patience and kindness. Thank you very much!

To all my friends, thank you for all the support, particularly on those days when work did not go as expected. Hey, one more stage reached!

Above all, I thank my family, who stood beside me, encouraged me constantly, and were able to provide me this experience.

Thank you, Gracias, Obrigada!

Não tenhamos pressa, mas não percamos tempo.

José Saramago

Get up, stand up, don't give up the fight!

Bob Marley and Peter Tosh

Abstract

The CD5 and CD6 lymphocyte surface receptors are highly homologous members of the Scavenger Receptor Cystein Rich (SRCR) superfamily mainly expressed by all T lymphocytes and the B1a subpopulation of B cells. Although the ultimate function/s are far from being completely understood, CD5 and CD6 are known to play a relevant role in both lymphocyte development and differentiation by negatively modulating the survival/death-inducing intracellular signals generated during the antigen recognition. Recently, this group has developed a transgenic mouse line which expresses a soluble form of human CD5, likely blocking the ligand-receptor interactions mediated by CD5 and interfering with normal lymphocyte response.

This study was aimed at furthering the study of the recombinant soluble human CD5 Transgenic (rshCD5Tg) mouse phenotypical analysis, its response to antigen stimuli and tumor implantation; the function of rshCD6 was also tested.

It was observed that rshCD5Tg mice display an exacerbated immune response, likely due to a reduction in the number of T and B cells with regulatory/suppressive function (Treg, B1a, B10 cells) and the increase in effector cells (NKT, MZ B cells). In agreement with these phenotypical characteristics, the functional analysis of rshCD5Tg mice showed enhanced immune responses to T-dependent and –independent antigens, as well as enhanced anti-tumoral responses, with or without concomitant chemotherapy treatment. Importantly, both the phenotypical and functional findings could be reproduced in wild-type mice following prolonged infusion of purified exogenous rshCD5 protein.

Overall, these results argue in favor of a relevant role of CD5-mediated molecular interactions in the homeostasis of functionally relevant lymphocyte subpopulations and open the possibility for CD5-based therapeutical interventions in different disease settings such as cancer, infection and immunodeficiency.

Keywords: Scavenger receptor cysteine-rich receptors; CD5/CD6 lymphocyte receptors; transgenic mice; tumor models; immunomodulation.

Resumo

Os receptores linfocitários de superfície, CD5 e CD6, são membros altamente homólogos da superfamília de receptores *Scavenger* ricos em cisteína (SRCR), que se expressam em todos os linfócitos T e na subpopulação B1a das células B. Apesar das funções de CD5 e CD6 ainda não estarem completamente determinadas sabe-se que têm um papel relevante no desenvolvimento linfocitário assim como na sua diferenciação modulando negativamente os sinais intracelulares de indução de sobrevivência/morte gerados durante o reconhecimento antigénico. Recentemente, o grupo desenvolveu uma linha de ratos transgénicos que expressam a forma solúvel humana de CD5, levando ao bloqueio das interacções receptor-ligando mediadas por CD5 e interferindo com a resposta linfocitária normal.

Este estudo teve como objectivo aprofundar a caracterização fenotípica do rato transgénico (rshCD5Tg) e a sua resposta a estímulos antigénicos e tumorais; a função de rshCD6 também foi testada.

Observou-se que o rato rshCD5Tg possui uma resposta imune exacerbada, provavelmente devido a uma redução do número de células B e T com função reguladora/supressora (células Treg, B1a, B10) e o aumento do número de células efectoras (células NKT e B da MZ). De acordo com estas características fenotípicas, a análise funcional do rato rshCD5Tg demonstrou uma resposta imune a antígenos T dependente e independente exacerbada, assim como uma resposta anti-tumoral aumentada, com ou sem tratamento quimioterapêutico concomitante. É ainda de referir que as descobertas tanto a nível fenotípico como a nível funcional podem ser reproduzidas em ratos WT após administração prolongada da proteína rshCD5 exógena purificada.

Em suma, estes resultados comprovam a importância das interacções moleculares mediadas por CD5 na homeostasia de subpopulações linfocitárias funcionalmente relevantes e torna possível a futura utilização de CD5 em intervenções terapêuticas em diferentes quadros clínicos, como por exemplo, cancro, infecção e imunodeficiências.

Termos-Chave: Receptores tipo *Scavenger* ricos em cisteína; Receptores linfocitários CD5/CD6; rato transgénico; modelos de tumores; imunomodulação.

List of Abbreviations and terms

- aa –amino acid
- Ab – Antibody
- Ag – Antigen
- ALCAM - Activated leukocyte cell adhesion molecule
- AOM - Azoxymethane
- APC – Antigen presenting cells
- BCR – B cell receptor
- bp – base pairs
- BSA – Bovine Serum Albumin
- CD – Cluster of Differentiation
- CD5L – CD5 ligand
- CFA - complete Freund's adjuvant
- DMSO - Dimethyl sulfoxide
- DNA - Deoxyribonucleic acid
- DSS – Dextran Sulfate Sodium
- ELISA - Enzyme-Linked ImmunoSorbent Assay
- FBS - Fetal Bovine Serum
- h – hour
- hCD5 – human CD5
- HSA – Human Serum Albumin
- i.p. – intraperitoneal
- i.v. - intravenous
- Ig - Immunoglobulin
- IL – Interleukin
- kb - Kilobases
- kDa – Kilodaltons
- KLH - Keyhole Limpet Hemocyanin
- LPS – Lipopolysaccharide
- MHC – Major Histocompatibility Complex
- min - minutes
- MZ – Marginal zone
- NK – Natural killer
- NKT – Natural killer T

- OD – Optic Density
- PAMP - Pathogen-associated molecular patterns
- PBS - Phosphate Buffered Saline
- PCR – Polymerase Chain Reaction
- PFA – Paraformaldehyde
- RNA - Ribonucleic acid
- Rpm – rotations per minute
- rshCD5 – recombinant soluble human CD5
- rshCD5tg – recombinant soluble human CD5 transgenic mice
- rshCD6 – recombinant soluble human CD6
- RT – room temperature
- s.c. – subcutaneous
- SD – Standard deviation
- SR – Scavenger Receptor
- SRCR - Scavenger Receptor Cysteine Rich
- SRCR-SF – Scavenger Receptor Cysteine Rich- Superfamily
- TCR – T cell receptor
- TD – T dependent
- TI – T independent
- TIL – Tumor Infiltrating Lymphocytes
- TLR – Toll-like receptor
- TNP - Trinitrophenyl
- Treg – regulatory T cells
- WT – Wild-type
- Zym – Zymosan
- β -GLU - β -glucan

Contents	Page:
Acknowledgements	I
Abstract	III
Resumo	V
List of Abbreviations and terms	VII
Table of Contents	IX
Index of Figures	XI
Index of Tables	XIII
1. Introduction	1
1.1. The Immune System	1
1.2. Specificity of the adaptive immune response	1
1.3. Antitumor Immunity	3
1.4. Scavenger receptors and SRCR Super-Family	4
1.5. Group B SRCR-SF members	5
1.5.1. CD6 molecule	5
1.5.2. CD5 molecule	7
1.5.2.1. CD5 expression in T cells	8
1.5.2.2. CD5 expression in B cells	8
1.5.2.3. Role of CD5 in the regulation of the TCR response	8
1.6. CD5 ligands	9
1.7. Recombinant soluble human CD5 transgenic mice	9
1.8. Objectives	12
2. Materials and Methods	13
2.1. Maintenance of the mice colony	13
2.2. Genotyping of mice	14
2.3. Validation of the results with transgenic mice injecting rshCD5 in wild-type mice	15
2.3.1. Confirmation of biological functionality of commercial lots of rshCD5 by ELISA	15
2.3.2. Confirmation of new lot functionality by a sepsis model	16
2.3.3 Detection of rshCD5 serum levels by ELISA after injection	17
2.4. Characterization of lymphocyte populations in mice	18
2.4.1. rshCD5 transgenic mouse	18
2.4.2. Effect of rshCD5 and rshCD6 injection in mice	19
2.5. Immunization with T-independent type 1 and 2 and T-dependent antigens	19
2.6. Experimental Tumor Models	20
2.6.1. B16 melanoma cell line	20

2.6.2. RMA-S lymphoma cell line	21
2.6.3. MCA 205 sarcoma cell line	21
2.6.4 Measurement of cytokines levels in tumor extracts by ELISA	22
2.6.5. AOM/DSS colon carcinogenesis murine model	22
2.7. Data Analysis	22
3. Results	23
3.1. Genotyping of mice	23
3.2. Validation of the results with transgenic mice injecting rshCD5 in wild-type mice	24
3.2.1. Confirmation of biological functionality of commercial lots of rshCD5 by ELISA	24
3.2.2. Confirmation of new lot functionality by a sepsis model	25
3.2.3 Detection of serum levels by ELISA after rshCD5 injection	27
3.3. Characterization of lymphocyte populations in mice	27
3.3.1. rshCD5 transgenic mouse	27
3.3.2. Effect of rshCD5 and rshCD6 injection in mice	30
3.4. Immunization with T-dependent and T-independent type 1 and 2 antigens	34
3.5. Experimental Tumor Models	38
3.5.1. Role of rshCD5 in tumor development	38
3.5.1.1. B16 melanoma cell line	38
3.5.1.2. RMA-S lymphoma cell line	40
3.5.1.3. MCA 205 sarcoma cell line	40
3.5.1.4. Measurement of protein cytokines in tumor extracts by ELISA	41
3.5.1.5. AOM/DSS colon carcinogenesis murine model	41
3.5.2. Role of rshCD6 in tumor development	42
4. Discussion	43
4.1. Functional study of rshCD5 in the homeostasis of regulatory and effector lymphocyte subpopulations	43
4.2. Study of the rshCD5Tg mice immune response to TD and TI antigens	46
4.3. Tumor models in rshCD5Tg mice	47
4.4. Conclusions and future perspectives to further this study	49
5. References	51

1. Introduction

Fig. 1.1. – Ag presentation by an APC to a T cell in the adaptive immune response and subsequent activation of the T cell.	1
Fig. 1.2. – T lymphocytes receptors and accessory molecules.	1
Fig. 1.3. – B-cell receptor complex.	3
Fig. 1.4. – Schematic representation of group B SRCR-SF members.	5
Fig. 1.5. – Schematic representation of the interaction between the membrane-bound and soluble forms of CD6 and its ligand, ALCAM.	6
Fig. 1.6. – Schematic representation of the interaction between the membrane-bound and soluble forms of CD5 and its ligand.	7
Fig. 1.7. – Summary of the observed and predicted changes in lymphocyte populations of rshCD5Tg mice.	11

2. Materials and Methods

Fig. 2.1 – Breeding schemes for different mouse genotypes.	13
--	----

3. Results

Fig. 3.1. – Illustration of agarose electrophoresis gels obtained from the DNA screening of rshCD5 transgenic and non-transgenic mice by PCR.	23
Fig. 3.2. – Western Blot confirming the biotinylation of a new batch of rshCD5 and BSA.	24
Fig. 3.3. – rshCD5 binding to different yeast wall components.	25
Fig. 3.4. – CD1 mice sensitivity to septic shock induced by zymosan.	25
Fig. 3.5. – Inflammatory response 18h after induction of septic shock by zymosan.	26
Fig. 3.6. – C57BL/6 WT mice sensitivity to septic shock induced by zymosan.	26
Fig. 3.7. – Inflammatory response 18h after induction of zymosan septic shock by zymosan.	26
Fig. 3.8. – Detection of exogenously administrated rshCD5 in C57BL/6 WT mice.	27
Fig. 3.9. – Flow cytometry analysis of $\gamma\delta$ T cells in rshCD5Tg and non-transgenic mice.	28
Fig. 3.10. – Percentage of $\gamma\delta$ T cells in lymphocytes.	28
Fig. 3.11. – Flow cytometry analysis of MZ cells in rshCD5Tg and non-transgenic mice.	29
Fig. 3.12. – Percentage of MZ cells in spleen lymphocytes (n=5) in 7/10 week old rshCD5Tg and non-transgenic mice.	29
Fig. 3.13. – Flow cytometry analysis of NKT spleen cells in rshCD5Tg mice.	30
Fig. 3.14. – Percentage of NKT spleen cells in 7/10 week old rshCD5Tg and non-transgenic mice (n=5).	30
Fig. 3.15. – Flow cytometry analysis of peritoneal Treg cells.	31
Fig. 3.16. – Percentage of peritoneal and spleen cell populations in 7/10 week old C57BL/6 WT mice (n=3).	32

Fig. 3.17. – Flow cytometry analysis of peritoneal B-1 cells.	33
Fig. 3.18. – Percentages of cell subpopulations in treated and control mice.	33
Fig. 3.19. – Hapten-specific antibody responses in rshCD5Tg and non-transgenic mice.	35
Fig. 3.20. – Percentage of spleen B-1 cells at day 21 post-immunization.	35
Fig. 3.21. – Hapten-specific antibody responses in rshCD5Tg and non-transgenic mice.	36
Fig. 3.22. – Hapten-specific antibody responses in rshCD5Tg and non-transgenic mice.	37
Fig. 3.23. – Percentage of spleen and peritoneal B-1 cells at day 14 post-immunization.	38
Fig. 3.24. – B16 tumor growth <i>in vivo</i> .	39
Fig. 3.25. – Effect of rshCD5 as a chemotherapy adjuvant.	39
Fig. 3.26. – RMA-S tumor growth <i>in vivo</i> .	40
Fig. 3.27. – MCA 205 tumor growth <i>in vivo</i> .	40
Fig. 3.28. – Murine IL-1 β , IL-6, IL-10 and TNF- α levels in tumor extracts by ELISA.	41
Fig. 3.29. – Number of colon tumors in mice treated with AOM/DSS.	41
Fig. 3.30. – Effect of rshCD6 as a chemotherapy adjuvant.	42
4. Discussion	
Fig. 4.1. – NKT cells express the surface marker of NK1.1 and a semiinvariant T cell receptor (TCR).	45

2. Material and Methods

Table 2.1. – Sequence of the specific pair of primers amplifying the extracellular region of human CD5.	14
Table 2.2. – Sequence of the specific pair of primers to the LIEX gene.	14
Table 2.3. – Recipe for SDS-PAGE gels.	15
Table 2.4. – Flow cytometry antibodies used in the study with the respective conjugate, work dilution and distributor.	18
Table 2.5. – Table of anti-Immunoglobulin antibodies used and their working dilutions for each experiment type.	20

1. Introduction

1.1. The Immune System

The immune system is responsible for defending the organism against foreign or self threats. This defense can be divided for its study into two types of immune response: innate and adaptive. The innate, natural or nonspecific immunity (phylogenetically the oldest defense system) is the first line of host defense for multicellular organisms and is a very fast response (almost in seconds through the first phases, 0 to 5 days). Innate immunity always responds similarly to the infection and the mechanisms of response are intrinsic (natural), not needing a prior exposure to the potentially harmful stimuli. This response consists on the one hand of soluble components such as complement molecules and cytokines, and on the other hand of cellular components such as macrophages, neutrophils, monocytes and NK lymphocytes. Actually, the innate response does not recognize specific pathogens but common structures of these pathogens which are essential to their survival and distinct from host molecules, and which are termed pathogen-associated molecular patterns (PAMPs).

When the defensive capacity of the organism grows with the increasing number of successive exposures to a particular pathogen, it is said that the response adapts to the threat – involving the adaptive, acquired or specific immunity. This response is only present in vertebrates and consists on the one hand of soluble components (humoral immunity) such as antibodies and cytokines, and on the other hand of cellular components such as B and T (cellular immunity) lymphocytes. Unlike the innate response, adaptive response is specific to the pathogen and may develop memory, so that in future contacts the response is improved. In order for B and T lymphocytes to be activated, it is necessary that they recognize and bind to the antigen (Ag). In some cases the Ag alone can activate the B cell, but mostly simultaneous activation by T cells (termed T helper cells) is necessary. When B lymphocytes are activated, they generate immunoglobulins, specific antibodies to the Ag recognized by the B cell receptor. Regarding T cells, there are many subpopulations with different functions and characteristics, but these cells are generally divided for their study in T helper (which promote cell response and Ab production) and T cytotoxic cells (which recognize the cells that express the Ag and lyse them).

This simplified breakdown of the immune system helps with the understanding of this complex organization, but in reality it is very difficult to establish defined boundaries between responses.

1.2. Specificity of the adaptive immune response

The specificity of the adaptive immune response lies in the antigen receptor on T and B cells, named TCR and BCR respectively.

The T lymphocytes recognize peptide fragments of Ag, but only in a certain context, and so these fragments must be presented by a specific cell - Ag-presenting cells (APC) that process the Ag

in order to be recognized by TCR. These cells must establish a stable contact to initiate the signal transduction in the T cell through the recognition of the Ag within the polymorphic structure of the Major Histocompatibility Complex molecule (MHC).

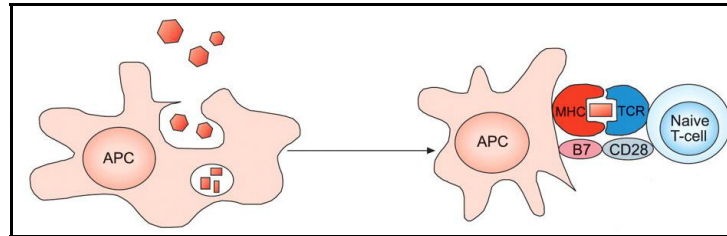


Fig. 1.1. – Ag presentation by an APC to a T cell in the adaptive immune response and subsequent activation of the T cell. APC: antigen-presenting cell; MHC: major histocompatibility complex; TCR: T-cell receptor. Adapted from Kallinich *et al.*, 2007.

Signaling triggered by Ag recognition is not effected through the TCR itself, but through accessory proteins such as CD3. These molecules are non-covalently linked to the TCR to form the TCR complex. There are more accessory molecules involved in the signal transduction processes, facilitating and improving, as well as downregulating, signaling to modulate the activation of the T lymphocyte and also to stabilize TCR-MHC binding (immunological synapse).

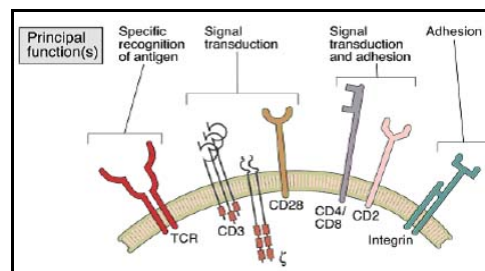


Fig. 1.2. –T lymphocyte receptors and accessory molecules. Adapted from Abbas *et al.*, 6th edition, 2008.

The TCR consists of a TCR α and TCR β dimer covalently bound with disulphide bridges. These are non-covalently bound to the transmembrane CD3 signalling complex, consisting of CD3 γ , CD3 δ , CD3 ϵ and CD3 ζ , which activate the T cell after Ag contact (Smith-Garvin *et al.*, 2009). The accessory molecule signals modulate the activation of the lymphocyte and may influence the type of response. Among these molecules, the most important are CD4, CD8, CD2, CD28 (signal amplification), CD11a, CD18, CD29 (pro-adhesive integrins), scavenger-like receptors (CD5 and CD6) and mucins (which have both an adhesive and signalling role).

The BCR is responsible for the survival of B cells thanks to the signals it provides to the cell. Antigenic recognition by the BCR is also needed for the activation of B lymphocytes. This activation is provided by the union of the Ag with the membrane IgD that is non-covalently associated with the Ig α and Ig β chains, which constitute the BCR complex. The Ig α and Ig β molecules, bound together by

disulfide bridges, are responsible for signal transduction, since the cytoplasmic tail of IgD and IgM is very short and lacks intrinsic catalytic properties. It can be said that these two molecules have a similar function to that of CD3 and ζ in T cells.

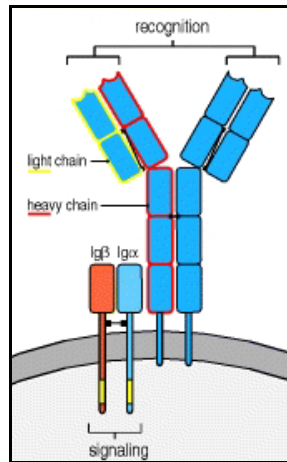


Fig 1.3. – B-cell receptor complex. Surface immuno-globulin associated to the invariant proteins Ig α and Ig β . The immunoglobulin recognizes and binds antigen and the Ig α and Ig β , which are antigen-nonspecific, are the signaling molecules. The latter possess a single immunoreceptor tyrosine-based activation motif (ITAM) each, shown as a yellow segment, in their cytosolic tails. Ig α and Ig β are disulfide-linked and associated with the heavy chains. Adapted from Janeway, C. A. Jr. *et al.*, 5th edition, 2001.

After their activation, B lymphocytes can follow two paths, interact with T lymphocytes (T-dependent response) or differentiate and proliferate regardless of T cells (T-independent response).

1.3. Antitumor Immunity

Cancer is the disease with the highest rate of mortality and morbidity among children and adults. It is defined by uncontrolled cell proliferation and possible spread of the transformed cells, involving invasion of adjacent/distant tissue (metastasis).

The immune system is able to recognize and destroy these malignant cells and to halt the development of tumors; however, a frequent characteristic of malignant tumors is their ability to escape or overcome the host's defense mechanisms.

There exists extensive information regarding the recognition of Ag expressed by tumors and antitumor immune response. Although tumor cells derive from the host, they express Ag that are recognized as foreign and trigger an immune response. On histopathological studies, it was observed that many tumors are surrounded by cellular infiltrates composed of T lymphocytes, NK cells and macrophages. However, the immune response is often ineffective against tumor growth, because the tumors are poorly immunogenic (they are derived from host cells and possess similar characteristics to other normal cells), grow/spread faster than the immune system can eradicate the tumor cells, or the tumor possesses specialized mechanisms to escape from the immune response (for example, they downregulate expression of tumor Ags, they are deficient in MHC class I expression or synthesize immunosuppressive proteins).

Tumor Ags may have different origins: they could be mutated host proteins (i.e., in tumors induced by radiation or carcinogens, for example) or expressed in an aberrant form/excess (as occurs in melanoma, for example).

The antitumor response may be carried out by innate and/or adaptive immunity. This type of response involves innate specialized cells such as NK cells and macrophages, as well as adaptive specialized cells such as CD8⁺ cytotoxic lymphocytes, CD4⁺ helper T lymphocytes and the Ab-producing B lymphocytes that generate tumor antigen-specific antibodies.

1.4. Scavenger receptors and SRCR Super-Family

The term scavenger receptor (SR) was initially applied to those receptors expressed by macrophages and able to uptake modified lipoproteins as well as pathogens. Nowadays, the term includes a vast number of cell surface and soluble glycoproteins involved in the recognition/endocytosis of polyanionic molecules, proteins, lipids, etc., from the host or from pathogenic structures. It should be noted that the proteins with SR functions have widely different structures, containing domains that include among others collagen, C-type lectin or scavenger receptor cysteine-rich (SRCR) domains, involved in pattern recognition (Sarrias *et al.*, 2004).

The SRCR domain is rich in cysteine residues and is the molecular signature of the SRCR superfamily (SRCR-SF), with more than 30 different proteins sharing a high degree of structural and phylogenetic conservation; however, the only single common characteristic shared by all proteins of the SRCR-SF reported so far is that they are all extracellular. The SRCR domain has approximately 100-110 amino acids and can be found in extracellular membrane receptors and also in soluble proteins. These proteins can be expressed in hematopoietic and non-hematopoietic cells (Sarrias *et al.*, 2004); among the first are proteins expressed in cells of the immune system, which generally play a role in the development of the immune system and in the regulation of the innate and adaptive immune response, while the second group includes proteins expressed in non-immune cells such as epithelial cells from gastrointestinal, genitourinary and bronchopulmonary tract, and even in hepatocytes (Aruffo *et al.*, 1997).

The SRCR-SF can be divided into two groups: A and B. The SRCR domains from group A proteins contain 6 cysteine residues and are encoded by at least two exons. Meanwhile, SRCR domains from group B proteins contain 6 to 8 cysteine residues and are encoded by a single exon. The cysteine residues within the SRCR domain form disulphide bonds between them with the following pattern: C1-C4 (absent in group A), C2-C7, C3-C8 and C5-C6 (Fenutría, 2011).

1.5 Group B SRCR-SF members

To date, 12 protein members of the group B of the SRCR-SF have been described; among these proteins are CD5 and CD6. The extracellular region of these proteins is composed exclusively of three group B SRCR domains. CD5 and CD6 are expressed as both membrane and soluble forms in thymocytes, T and B1a lymphocytes (Sarrias *et al.*, 2007), where they modulate signaling through the TCR (both CD5 and CD6) and BCR (CD5 only), thus influencing host defense and homeostasis of the immune system. The human CD5 gene is localized in 11q12.2 chromosome, 82kb downstream from the human CD6 gene; these genes are also located in a similar position in mice chromosome 19 (Aruffo *et al.*, 1997; Arman, 2004). The conserved loci of those genes, both in human and mouse, supports the theory that these two genes may have evolved from duplication of a primordial gene.

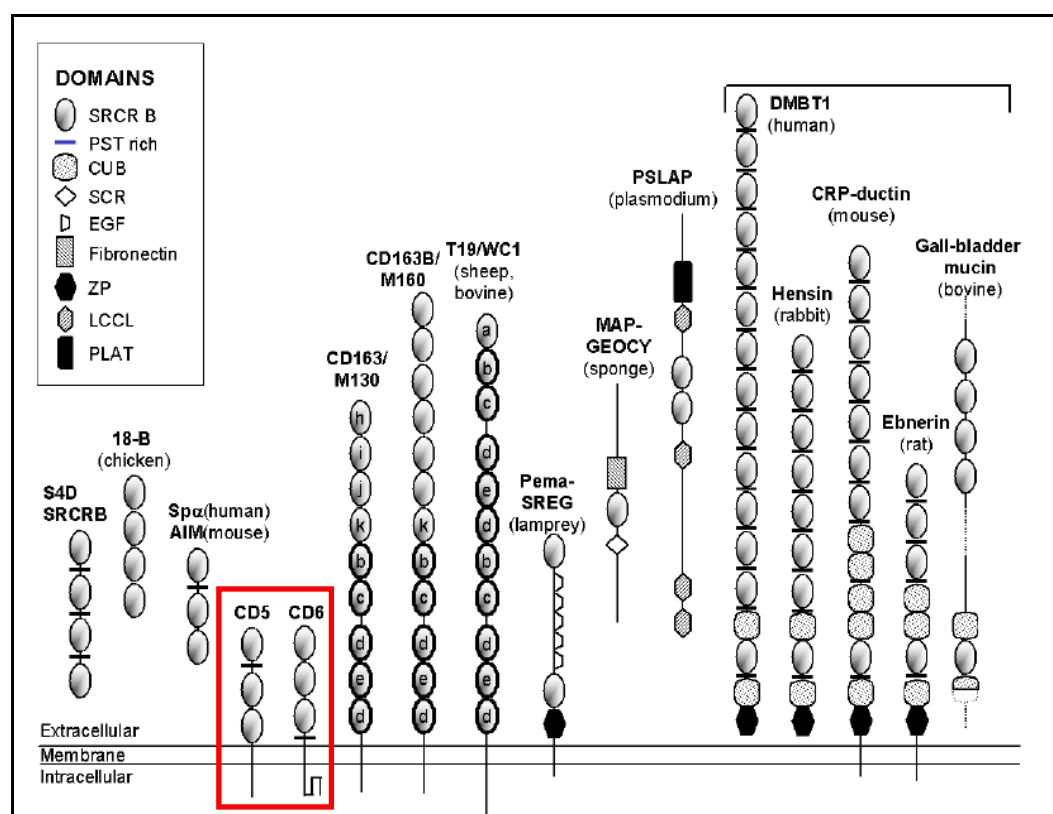


Fig. 1.4. – Schematic representation of group B SRCR-SF members. Proteins described in mammals, unless indicated. In the red rectangle are the members of this family studied in this work. Adapted from Sarrias *et al.*, 2004.

1.5.1 CD6 molecule

CD6, an SRCR-SF group B membrane receptor, is a 100 to 130 KDa type 1 membrane glycoprotein, highly glycosylated and with an expression pattern and structure greatly similar to CD5 (Sarrias *et al.*, 2004). Several isoforms, so far 5, have been reported which only differ in the length of the cytoplasmatic region (24 to 244 aa) resulting from alternative RNA splicing (Aruffo *et al.*, 1997). The intracellular tail lacks intrinsic enzymatic activity but can participate in signal transduction events, and consists of 24 to 244 aa, with the heavy isoform being the most common. The

transmembrane region consists of 26 aa and the extracellular region is composed of 3 SRCR domains (homologous to the corresponding domains of CD5) followed by a spacer region of 33 aa, resulting in a highly glycosylated molecule with a length of 374 aa (Bowen *et al.*, 2000).

As described above, this molecule is expressed in thymocytes, mature T cells, and B1-a cells, similar to CD5, but also in brain: cerebral cortex and basal ganglia, and also in chronic B-cell lymphocytic leukemias (Arman, 2004). CD6 is associated and co-localizes with CD5 in the membrane of resting T lymphocytes and in the immunologic synapse during the cellular activation. Following this activation, CD6 levels are up-regulated.

CD6 is a co-stimulatory molecule that enhances the development and differentiation of mature T cells, modulating the TCR signaling by synergizing with other co-stimulatory molecules and proliferative signals of the TCR (Arman, 2004). Furthermore, it has also been described that membrane and soluble forms of CD6 can bind to Gram-positive and Gram-negative bacteria through the recognition of PAMPs such as LPS and LTA, a function shared with other members of the ancient and highly conserved SRCR-SF (Soldevila *et al.*, 2011). The soluble form is thought to be originated by a proteolytic cleavage process but it is still uncertain. Also, there is virtually no information regarding its physiological function/s, save from the fact that they are able to bind CD166/ALCAM as well as pathogens through PAMPs.

Different CD6 ligands have been reported, but the main ligand for this receptor is ALCAM (activated leukocyte-cell adhesion molecule). This type 1 membrane glycoprotein of the Ig superfamily is expressed in activated leukocytes (T and B), monocytes, neurons and thymic epithelium (Arman, 2004). The specific CD6/ALCAM binding takes place through the SRCR-D3 and the N-terminal V-like Ig domain with a 1:1 stoichiometry (Arman, 2004; Sarrias, 2004). The CD6 binding site on human and murine ALCAM is conserved, allowing for cross-species binding activity.

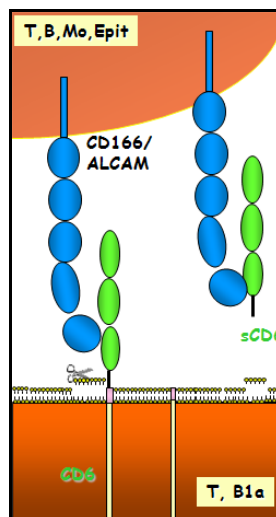


Fig. 1.5. –Schematic representation of the interaction between the membrane-bound and soluble forms of CD6 and its ligand, ALCAM. Adapted from Sarrias *et al.*, 2007.

1.5.2 CD5 molecule

CD5, also known as T1, Leu-1, Tp67 (human) or Ly-1 (mouse), is a 67KDa type 1 membrane glycoprotein (Sarrias *et al.*, 2004). The extracellular region is composed of 3 SRCR domains, where domains 1 and 2 are separated by a proline-threonine-rich region and domain 2 and 3 are directly linked in tandem (Bowen *et al.*, 2000), for a total of 350 aa; the transmembrane region is composed of 31 aa and the cytoplasmic region, highly conserved and with 90% homology between human and mouse, 92 aa (Fenutría, 2011). Domain 1 (SRCR1), the furthest from the cellular membrane, is the less conserved as compared to other mammalian SRCR domains and the most immunogenic (Arman, 2004). SRCR1 and SRCR2 are the domains involved in the interaction with the putative CD5 ligand, while SRCR3 is important in stabilizing this interaction (Calvo *et al.*, 1999).

The first protein of the SRCR-SF described to have a soluble form was CD5. This form has a molecular weight of 52KDa and can be found circulating in serum at low levels, and probably results from proteolytic cleavage after lymphocyte activation (Arman, 2004; Fenutría, 2011), but their functional relevance has not yet been fully investigated. Elevated levels of this protein have been found in certain autoimmune diseases suggesting that shCD5 may be an indicator of chronic or exacerbated T cell activation, or alternatively, that it may play a role in the modulation of the immune response by interacting with CD5 ligand/s.

As mentioned above, CD5 is expressed in thymocytes, T and B1a lymphocytes and also in macrophages and dendritic cells (Fenutría, 2011). It is an accessory molecule capable of modulating activation and differentiation signaling through the TCR and BCR by physical association with the TCR/CD3 complex (also associated with the surface receptors CD4, CD8, CD2, CD6, CD9) and the BCR (Lozano *et al.*, 2000). In this way, it is possible to affirm that CD5 is an important regulatory molecule in the responses mediated by B and T lymphocytes, which is supported by the fact that the expression of CD5 is up-regulated following TCR-CD3 crosslink and murine B-IgM crosslink. However, this molecule has been described as a positive but also negative modulator of the activation and differentiation signals received from the Ag-specific receptor on diverse cell types and development stages, as will be described later.

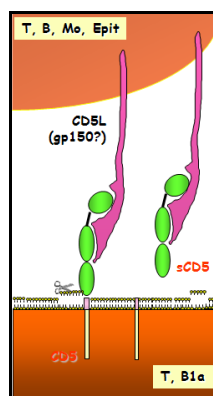


Fig. 1.6. – Schematic representation of the interaction between the membrane-bound and soluble forms of CD5 and its ligand. Adapted from Calvo *et al.*, 1999.

1.5.2.1. CD5 expression in T cells

CD5 membrane expression is highly regulated throughout T development/maturation in the thymus, which makes CD5 a highly specific marker of T lymphocytes (Arman, 2004; Fenutría, 2011). The immature double negative thymocytes have the lowest levels of CD5, which increase with the activation of the pre-TCR. This increase continues with the transition to double positive thymocytes and positive selection and conversion to single positive T lymphocytes; CD5 levels are higher in CD4⁺ single positive than in CD8⁺ single positive T lymphocytes. However, the levels of CD5 may vary in mature peripheral T cells, depending on the TCR avidity for the antigen developed during thymic selection (the higher the TCR avidity, the higher the CD5 expression) (Sellick *et al.*, 2008). As a result, CD5 levels are highest in one particular type of regulatory T cells with a CD4⁺CD25⁺FoxP3⁺ phenotype, which possess very high affinity TCRs and maintain immune tolerance. As for CD8⁺ cells, it has been reported that the levels of CD5 are elevated when they are chronically exposed to an Ag, but return to basal levels outside that environment (Stamou *et al.*, 2003).

1.5.2.2. CD5 expression in B cells

CD5 expression in B CD5⁺ cells is much lower than in T CD5⁺ cells. In human peripheral blood, B CD5⁺ cells represent 1% of all lymphocytes and 10-15% of total B cells. In mice, CD5 expression can only be detected in a particular subtype, the B1a cells, characterized by a CD5⁺CD23⁻IgM^{high}IgD^{low} phenotype and hosted mostly in the peritoneal cavity, where they represent 30 to 60% of total peritoneal cavity cells (Baumgarth, 2011). This subtype was originally thought to be of fetal origin because of the expression of a T cell marker, but is now known to differ from the B2 or conventional B cells in both phenotype (conventional B cells are IgM^{low}IgD^{high}CD23⁺CD5⁻) and function. When comparing these two subpopulations, the B1a cells are more longevous and appear to be important for T cell-independent type 2 cell responses (Martin *et al.*, 2001), as well as generating natural IgM (natural polyreactive Abs with low affinity) that eliminate bacterial toxins and allow effective resistance to pathogens as part of the innate immune response (Baumgarth, 2011). This subpopulation also shows lower BCR affinity and diversity than B2 cells.

1.5.2.3. Role of CD5 in the regulation of the TCR response

The cytoplasmic tail of CD5 does not possess intrinsic catalytic activity, but has potential sites for phosphorylation by intracellular kinases, so that it is able to modulate the activity of adjoining signaling proteins. CD5 is physically associated to the TCR, and when this is activated by an Ag, CD5 is one of the first proteins to be phosphorylated.

The first functional assays performed to study the function of CD5 in peripheral T cells *in vitro* indicated that this molecule acted as a co-stimulator, enhancing the proliferative response resulting from the activation of the TCR/CD3 complex (Alberola-Ila *et al.*, 1992; Verwilghen *et al.*, 1993).

However, later studies with CD5 knockout mice showed that CD5-deficient mature T lymphocytes presented an exacerbated response to the TCR signalization/stimulation, suggesting that this molecule acted as a negative regulator of the TCR (Bikah *et al.*, 1996; Pena-Rossi *et al.*, 1999). Furthermore, the knock-down of CD5 levels was sufficient to reestablish the proliferation of a subpopulation of B lymphocytes, B1a cells; this indicates that the signals mediated by the BCR might be negatively regulated by the CD5 present in these cells.

1.6. CD5 ligands

A lot of controversy exists around the issue of the CD5 ligand/s. At present, CD5 ligand/s are still unknown, but a lot of candidates have been described: CD72, gp3440, gp40-80, gp150 and even CD5 itself (Brown and Lacey, 2010; Soldevilla *et al.*, 2011), among others. The reason the ligand of CD5 is still unknown may be due to the fact that it is an unstable molecule with high conformational flexibility. However, more work is currently underway for the identification of the ligand of CD5, as its discovery would help to further the existing knowledge on the CD5 function.

The first reported ligand was CD72, a type C lectin expressed in B lymphocytes; however, no other research group was able to reproduce these results (Velde *et al.*, 1991; Calvo *et al.*, 1999). An interaction between CD5 and other proteins expressed on the surface of B cells such as gp200, gp40-80, etc., was later described, which might indicate a role for CD5 in the cooperation between T-B and B-B lymphocytes (Arman, 2004). Another described ligand was gp150, expressed in monocytes, lymphocytes, thymic epithelium, etc.; this interaction could explain the participation of CD5 in the APC-T cell interaction, the activation of T cells and the development and maturation of the thymocytes (Calvo *et al.*, 1999).

Further studies are necessary to define which is the true ligand of CD5 and what is the functional importance of the CD5-CD5L interaction.

1.7. Recombinant soluble human CD5 transgenic mice

There exist various issues concerning the complex and controversial function/s of CD5, but it is clear that this molecule has the potential to be a key player of the immune system, modulating both the development of immune cells and the immune response. In order to further the knowledge of CD5, the group where this work was developed generated a transgenic mouse expressing the human soluble form of CD5, termed the rshCD5Tg mouse. As previously mentioned, the function of the soluble form of CD5 remains unknown to date, but this mouse would also shed light on the functional importance

of the CD5-CD5L interaction. In this way, it would help to clarify the functions and role of CD5 in the immune system.

A practical advantage of this mouse model was the continuous endogenous production of rshCD5 with the aim of saving on production and purification of protein for administration; this would also eliminate the stress mice experiment at repeated injections. More importantly, the circulating rshCD5 could interact with endogenous murine ligand/s, blocking the interaction of these ligands with membrane CD5 and thus inhibiting the processes dependent on this union. In this way, these mice are effectively deficient in those functions of CD5 dependent on the interaction of this receptor with his ligand. Inactivation or knock-down of CD5 function observed in these mice would not be due to gene inactivation or deletion, but would be just a functional effect mediated by the inhibition of the CD5-CD5L interaction. Another great advantage of this model is that potential beneficial results observed in it can be easily transferred to a possible treatment in humans by administration of recombinant protein, rather than gene inactivation or increase of gene expression, which in a patient is technically much more difficult than to administer purified exogenous rshCD5 (Fenutría, 2011).

Phenotypical analysis of the transgenic mice revealed that the presence of rshCD5 in serum has consequences on the dynamics of certain regulatory and effector lymphocyte subpopulations. Compared to C57BL/6 wild-type (WT) mice, the rshCD5Tg mice possessed the same total number of lymphocytes in thymus, lymph nodes, spleen and peritoneal cavity, as well as the same number of CD4 and CD8 single positives, double positives or double negatives, pre/pro B, early/late pro B, and follicular I and II B cells. The main differences observed were focused in subpopulations that express CD5, such as B1a, B10 (which negatively regulate the immune response in murine models of inflammation and autoimmunity) and Treg cells; all these subpopulations were reduced in transgenic as compared to non-transgenic mice. Finally, another subpopulation analyzed was NKT cells but in this case it was increased in rshCD5Tg mice as compared to non-Tg mice. The mechanism(s) through which CD5 regulates the number and proportion of cells within the regulatory subpopulations is unknown, but it probably involves the blocking of the CD5-CD5L interaction, which somehow modifies the cellular homeostasis and consequently the survival of these subpopulations. Importantly, the observed alterations in the dynamic of the aforementioned subpopulations was reproduced by repeated administration of rshCD5 (25 µg every 48h for two weeks) in C57BL/6 WT mice (Fenutría, 2011).

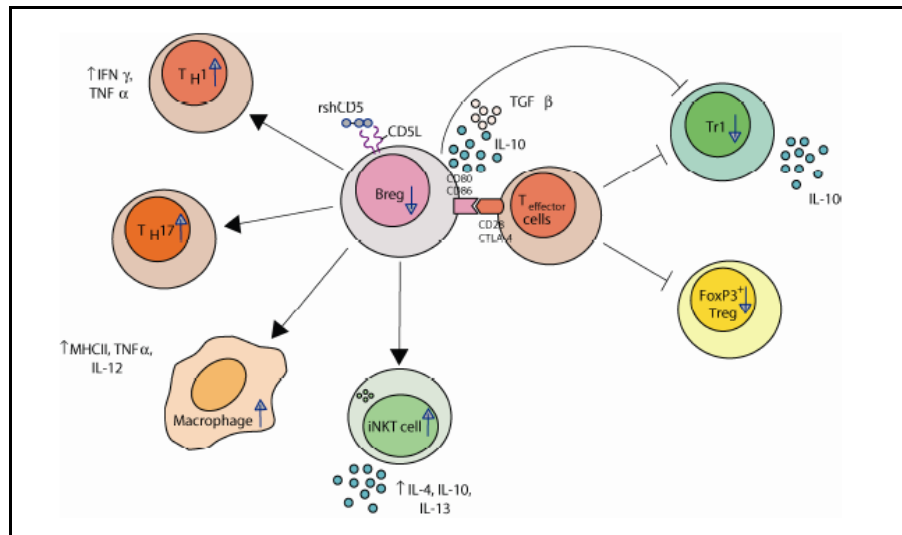


Fig. 1.7. – Summary of the observed and predicted changes in lymphocyte subpopulations in rshCD5Tg mice. The diagram shows how a decrease in the Breg subpopulation, associated with a decline in T regulatory population (FoxP3⁺Treg and Tr1), would affect the activity of T effector (Th1, Th17, NKT) subpopulations and macrophages. Adapted from Fenutria, 2011.

The decrease in subpopulations with regulatory/suppressive function, coupled with the increase in subpopulations with effector function, observed in rshCD5Tg mice suggested that the immune response might be enhanced in these mice as compared to non-transgenic mice. However, none of the differences observed were dramatic, which could lead to think that they would not be sufficient to have functional relevance. In order to confirm this, the response of the transgenic mice was analyzed in cases of autoimmune diseases and inflammation.

With regard to autoimmune diseases, the behavior of the transgenic mice was studied following induction of Experimental Autoimmune Encephalomyelitis (EAE) and Collagen-induced arthritis (CIA). It was found that the rshCD5Tg mice had a more exacerbated immune response than the C57Bl/6 WT mice (Fenutria, 2011).

To analyze the response of the rshCD5Tg mice in an inflammatory process, a model of fungal sepsis termed Zymosan-induced generalized inflammation (ZIGI) was used (Goris *et al.*, 1986). Zymosan (Zym) is a substance derived from the cell wall of yeast, specifically *Saccharomyces cerevisiae*, and it is composed of polysaccharide chains with various molecular weights; this compound is highly immunogenic. Following intraperitoneal administration of this substance, mice develop a systemic inflammatory condition at around 18 hours, and within 1-2 weeks a multiorgan dysfunction settles in, and the subsequent damage leads to the animal's death. In this model, the rshCD5Tg mice showed an improvement compared to the WT mice. Also, when C57Bl/6 WT mice were administered a single dose of CD5, prophylactic (1h before the Zym challenge) or therapeutic (1 or 3h after the Zym challenge), an improvement in the inflammatory process was observed compared to the control mice treated with BSA (Vera *et al.*, 2009). This result couldn't be explained only by the change in the subpopulation dynamics, which cannot be achieved with a single administration of rshCD5, but through another mechanism of action, later found to be the ability of rshCD5 to bind and

aggregate pathogens and their components, including β -glucan, a component of the fungal wall and consequently of Zym.

Due to its ability to modulate signaling through the Ag receptor of T and B lymphocytes, as well as its capacity to bind pathogens and their components, it can be said that CD5 is at the interface between innate and adaptive immunity. The modulation of inflammatory phenomena by CD5 suggests that there exist potential therapeutic uses for soluble forms of CD5 in different clinical situations requiring an enhancement of the immune response, such as tumors, vaccine therapy and immunodeficiency caused by disease or immunosuppressive therapy.

1.8. Objectives

The global aim of this project was to analyze and to improve the understanding of the immunomodulating role of the CD5 and CD6 lymphocyte receptors – and their interactions with their ligands - on the immune response.

In this context, the following specific objectives were defined:

- to further the knowledge of the potential consequences of the presence of circulating rshCD5 in mice serum in the dynamics of regulatory and effector lymphocyte subpopulations in normal conditions or in situations of immune stimulation;
- to carry out studies on different experimental models of disorders where the immune system is involved, such as tumors or infection, in rshCD5Tg mice or in non-transgenic mice following administration of an exogenous soluble recombinant form of human CD5 or CD6 (rshCD5 and rshCD6);
- to set the basis for future immune-mediated therapies aimed towards the blocking or synergizing the intracellular signals mediated by CD5 and/or CD6 in tumoral or infectious processes.

2. Materials and Methods

2.1. Maintenance of the mice colony

All protocols performed were approved by the Ethics Committee of the University of Barcelona and were performed in accordance with institutional guidelines for the Care of Animals that are included in the Spanish Legislation (RD 1201/2005), European (86/609) and American (National Institutes of Health's Guide for the Care and Use of Laboratory Animals).

For the experiments carried out, groups of mice were used with the highest possible N and similarities in age, sex and weight. For this purpose the following breeding strategy was established:

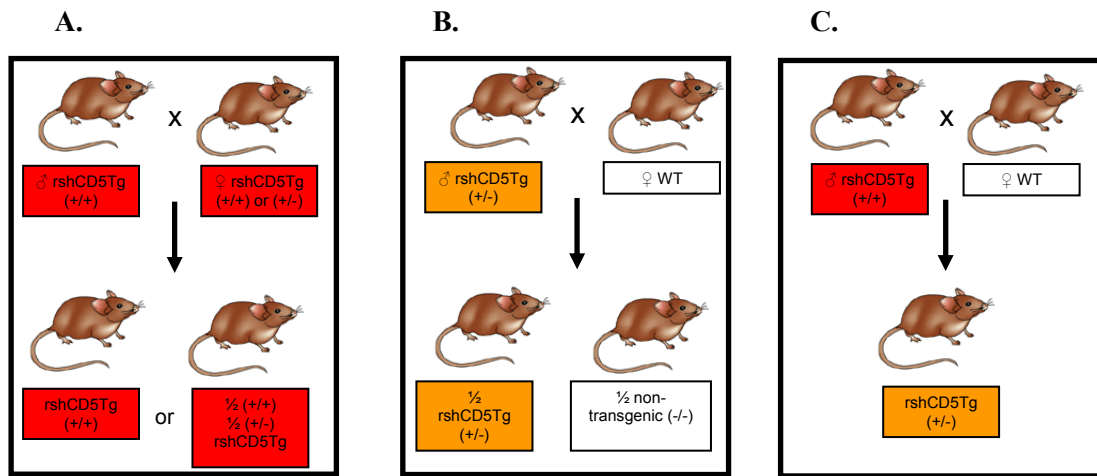


Figure 2.1 – Breeding schemes for different mouse genotypes. **A.** Breeding between a rshCD5 homozygote male and a transgenic female (homozygote or heterozygote) and the correspondent offspring. **B.** Breeding between a rshCD5 heterozygote male and a C57BL/6 WT female and the correspondent offspring. **C.** Breeding between a rshCD5 homozygote male and a C57BL/6 WT female and the correspondent.

For the experiments, both transgenic and non-transgenic (control) littermate mice were needed, so 3 cages were set up according to breeding scheme **B.**, with one male and two females to obtain the maximum number of mice for these groups. Likewise, two cages were set up following breeding scheme **C.** (one male and two females each cage) to guarantee the existence of transgenic mice in the colony, while one cage (one male and two females) was set up according to breeding scheme **A.** to obtain homozygote males. To verify that males were homozygote, they were crossed with C57BL/6 WT females and their offspring was genotyped; the mouse was deemed homozygote if all the offspring was positive for the transgenic gene. These males were then used to substitute the homozygote males in the crosses after a certain period of time.

Once a week the colony was reviewed in order to organize the crosses, check the health of the mice and the number of new born mice, and to follow their development up to 4 weeks, when they are weaned and genotyped.

2.2. Genotyping of mice

To identify which mice were transgenic for rshCD5 a PCR was performed. Genomic DNA was extracted from an ear punch sample with 50µL of lysis buffer (1M Tris pH=8, 0,5M EDTA, 5M NaCl and 10% SDS) plus 1µL of proteinase K (Roche, Germany). Two pairs of Primers were used for each PCR (all provided by Sigma-Aldrich, USA), one specific for the transgene (the extracellular region of human CD5):

Table 2.1 – Sequence of the specific pair of primers amplifying the extracellular region of human CD5.

Forward Primer: CD5 ExtraFort	5'-GCTGTCCCAGTGCCACGAACTT-3'
Reverse Primer: PingSV40 poly A-R	5'-GAAGCTCCTCTGTGTCCTCAT-3'

originating one fragment of 450bp; and one for an internal PCR amplification control amplifying the LIEX gene (region of the invariant chain Li of MHC class I), present in all C57BL/6 mice, originating a fragment of 150bp:

Table 2.2 – Sequence of the specific pair of primers to the LIEX gene.

Forward Primer:	5'-TCACTCAAGGCAACCTTCCTGC-3'
Reverse Primer:	5'-CGACCTCATCTCTAACCATGAACAG-3'

PCR reactions were carried out in a final volume of 50µL, using 200uM of each dNTP, 300nM of each primer, 1x of Expand High Fidelity buffer (1,5mM MgCl₂), 2,6U of Expand High Fidelity enzyme mix and 1µL of DNA solution. Amplification was performed in a GeneAmp PCR System 2700 thermocycler (Applied Biosystems) using 30 cycles of 5min. at 94°C, 1min. at 92°C, 1min. at 53°C, and 8min. at 72°C.

To visualize the products of amplification, these were separated in a 2% agarose gel in 1X TBE buffer (89mM Tris-HCl, 89mM Boric Acid, 2mM EDTA pH=8, to a final volume of 1L distilled water) to which was added a 10,000x dilution of Syber Safe (SYBR® Safe DNA gel stain, Invitrogen) as suggested by the manufacturer. The molecular weight marker used was 1Kb Plus DNA ladder (Invitrogen, USA). Samples (15µL) were prepared before loading by the addition of 4µL of Blue Juice (Invitrogen, USA). Electrophoresis was carried out at 100V for 30min. The bands were visualized on the G:Box (SynGene) and the images obtained from the GeneSnap (SynGene).

2.3. Validation of the results with transgenic mice by injection of rshCD5 in wild-type mice

2.3.1. Confirmation of biological functionality of commercial lots of rshCD5 by ELISA

The rshCD5 used in these experiments was purchased from PX'Therapeutics (France) and whenever a new batch was started, tests were performed to ensure biological functionality. Below are described the tests carried out upon the arrival of a new batch.

Firstly, an aliquot of the new batch of rshCD5 and BSA (Sigma-Aldrich, USA) were biotinylated. For these experiments, EZ-Link[®] Sulfa-NHS.LC-LC-Biotin with a MW = 669,75 and spacer arm of 30,5Å (Pierce, Thermo Fisher Scientific, USA) was used. For labeling with biotin, the protocol provided by the manufacturer was followed, dissolving biotin in PBS at a concentration of 10mM and a ratio of 1:20 (protein: biotin). Once the protein was biotinylated, it was purified by desalting (HiTrap, GE Healthcare Biosciences, USA), removing the excess of biotin unbound to protein. Finally the proteins were quantified by spectrophotometry at 280nm (Gen5 1.09, Epoch, BioTek).

After purifying these biotinylated proteins, biotinylation was checked by Western Blot. First, the samples were separated by a SDS-PAGE gel electrophoresis (see table 2.3) in running buffer pH=8,3 (Tris HCl 25mM, Glycine 192mM and 0,1% SDS) at 100V until the dye front reached the bottom of the gel.

Table 2.3 – Recipe for SDS-PAGE gels.

Running Gel	distilled water = 4,4mL
	Tris pH=8,8 0,2%SDS = 10mL
	Acrylamide (Bio-rad, USA) = 5,6mL
	APS = 100µL
	TEMED (Bio-rad, USA) = 28µL
Stacking Gel	distilled water = 3,2mL
	Tris pH=6,8 0,2%SDS = 1,25mL
	Acrylamide (Bio-rad, USA) = 525µL
	APS = 25µL
	TEMED (Bio-rad, USA) = 5µL

The proteins were then transferred to a nitrocellulose membrane at 400A and 100V for 90min in freshly made transfer buffer (1,92M glycine, 0,25M Tris Base, 20%MeOH in distilled water). Afterwards, the membrane was blocked in 5% milk for 1h and then incubated with a 1/1000 dilution

of Streptavidin-POD Conjugate in blocking solution for 20min. After 3 washes with PBS-0,01%Tween 20, biotinylated proteins on the membrane were detected with SuperSignal[®] West Dura Extended Duration Substrate for a minute in the dark. Images were analyzed and recorded with the Luminescent Image Analyzer – ImageQuant LAS 4000.

Once the biotinylated proteins were checked, a Sandwich ELISA was performed to evaluate whether the new batch of rshCD5 bound to the yeast wall components *in vitro*.

A 96-well flat-bottom plate was coated with 2µg/mL of Zymosan (Sigma-Aldrich, USA), Mannan (Sigma-Aldrich, USA) or B-D-Glucan (Sigma-Aldrich, USA) (in a final volume of 100µL) in carbonate/bicarbonate buffer pH 9,5 overnight at 4°C. The coating solution was removed and the plate washed three times with PBS-0,05% Tween 20, then blocked for 1 hour at RT with 100µL of PBS-3% BSA (Sigma-Aldrich, USA). The supernatant was discarded and the plate washed three times. After these washes, each yeast wall component was incubated for 2h at RT with three different proteins/conditions: increasing concentrations {0; 0,05; 0,1; 0,5; 1; 2}µg/well of rshCD5-biotin from an already checked lot as positive control, BSA-biotin as negative control and rshCD5-biotin from the new lot, all in duplicate. The plate was washed again three times and after that incubated 30min at RT with a 1/1000 dilution of Streptavidin-POD Conjugate (Roche Diagnostics) in blocking solution. The plate was washed again three times and 100µL of TMB Substrate Reagent Set (BDOptEIA, BD Bioscience) were added to each well and incubated 10min in the dark. At this point, 100µL 0,5M Sulfuric Acid were added to each well to stop the reaction and the OD was measured in an ELISA reader (Gen5 1.09, Epoch, BioTek) at a wavelength of 450nm. It should be noted that another negative control was done using 1µg/well of rshCD6-biotin. A positive and negative control of the technique were also carried out by sensitizing the plate with already checked rshCD5-biotin or with buffer alone, respectively.

Two independent experiments were carried out for each new protein lot.

2.3.2. Confirmation of new lot functionality by a sepsis model

Besides the *in vitro* assays, an *in vivo* assay was also performed in the form of a sepsis model, Zymosan-Induced Septic Shock-Like Syndrome, already described by the group (Vera *et al.*, 2008).

In this experiment besides the CD1 mice (Charles River, Milan, Italy) mentioned in the article, 7/9 weeks old C57BL/6 mice (Charles River, France) were also used, weighing approximately 20g. Mice were injected i.p. with Zym 500mg/Kg (Sigma-Aldrich, USA) in 200µL of PBS. A single dose of 25µg of rshCD5 (or BSA as control) was administered one hour before administration of Zym (-1h). Then, 18 hours after injection of Zym the severity of septic shock was analyzed, using a clinical score from 0 to 3 (0 - no symptom, 1 - weak symptoms, 2 - moderate symptom, 3 - severe symptoms) characterizing septic shock parameters such as lethargy, diarrhea, conjunctivitis and hackles. The

values for each of the four parameters of each mouse were summed up to give an assessment of the severity or final score per mouse of septic shock. The levels of cytokines were also analyzed at 18 hours post Zymosan-Induced Septic Shock. For cytokine detection in serum, the mice were euthanized by an overdose of Isoflurane and the blood extracted by cardiac puncture.

For detection and quantification of cytokines (murine IL-6 and IL-1 β) in the mouse serum, the ELISA BD OptEIA Kit (BD Biosciences) was used according to the manufacturer's instructions. Firstly, 96-well flat-bottom plates were sensitized overnight at 4°C with capture Abs for both cytokines diluted in 100 μ L of carbonate buffer at a dilution specified by the manufacturer. The next day the plates were washed three times with washing buffer (PBS 0.05% Tween-20) and blocked with blocking buffer (PBS-10% inactivated FBS) for 1h at RT. Once the plates were washed, 100 μ L of sample (diluted 1:30 in blocking buffer for IL-6, undiluted for IL-1 β) and the standards were added to each well in duplicate and incubated 2h at RT. After incubation, the plates were washed five times with washing buffer and 100 μ L of a solution containing the detection Ab plus the Streptavidin-POD Conjugate (Roche Diagnostics) in blocking solution were added at the indicated dilution for each cytokine Ab and incubated 1h at RT. After this incubation, the plate was washed 5 times with washing buffer and 100 μ L of TMB were added, incubating the plate 15/30 min at RT in the dark. To stop the reaction, 100 μ L of 2N sulfuric acid were added to each well and absorbance was measured at a wavelength of 450nm in the Gen5 1.09, Epoch, BioTek. The concentration of cytokines in the samples was calculated with a standard curve generated from the standards of known concentrations provided with the kit.

2.3.3 Detection of rshCD5 serum levels by ELISA after injection

These experiments were also carried out with a Sandwich ELISA to detect the serum rshCD5 level injected through time. Each 8 week female C57BL/6 WT mice were injected with 25 μ g of rshCD5 and blood samples were extracted at 0h, 1h, 3h and 6h. The blood was immediately placed on ice until centrifugation at 5000rpm at 4°C for 15min. The serum was collected and kept at -80°C until the trial.

The plate (96-well flat-bottom plate) was coated with the capture antibody CRIS-1 at a concentration of 0,5 μ g/ μ L (in a final volume of 100 μ L) in carbonate/bicarbonate buffer pH 9,5 (0.1M sodium carbonate) and incubated overnight at 4°C. The coating solution was removed and the plate washed three times with PBS-0,05% Tween 20. Blocking was carried out for 1 hour at RT with 100 μ L of PBS-5% inactivated FBS. After the incubation, blocking was discarded and the plate washed three times, then incubated with 100 μ L of the serum samples in duplicate, undiluted, for 2 hours at RT. A standard curve was also performed with serial rshCD5 dilutions (from 0 μ g/ μ L to 0,02 μ g/ μ L) in blocking solution in duplicate. The plate was washed again three times and then incubated with 100 μ L of

biotinylated LEU-1 at 2µg/mL for 1 hour at RT. Again, it was washed three times and incubated for 30min at RT with 100µL of 1/1000 dilution of Streptavidin-POD Conjugate (Roche Diagnostics) in blocking solution. After another 3 washes, 100µL of TMB Substrate Reagent Set (BD OptEIA, BD Bioscience) were added to each well and incubated 15min at RT in the dark. At this point, 100µL 2N sulfuric acid were added to each well to stop the reaction and the OD measured in an ELISA reader (Gen5 1.09, Epoch, BioTek) at a wavelength of 450nm. It should be noted that a control of the secondary Ab was also carried out by sensitizing the plate with 2µg/mL of biotinylated LEU-1 and treating it as the other samples.

2.4. Characterization of lymphocyte populations in mice

2.4.1. rshCD5 transgenic mouse

For the studies of lymphocyte populations by flow cytometry, the mice were euthanized with Isoflurane and the extracted tissues (spleen, thymus) or peritoneal lavage from rshCD5Tg and non-transgenic mice preserved on ice until the samples were processed. Flow cytometry was performed with a FACS Canto I flow cytometer (BD Biosciences, USA).

Firstly, cell suspensions were obtained (by mechanical tissue dissociation, if necessary) in PBS. Erythrocytes were then lysed by 5 min incubation at 4°C with NH₄Cl 0,16M and 1x10⁶ cells per mouse collected and blocked with PBS-10% inactivated FBS for 10min at 4°C. Then the samples were stained with the appropriate antibodies for each study (see table 2.4) for 30min. at 4°C. Treg lymphocyte populations require intracellular staining, which was performed following the instructions of the kit (PE anti-mouse/rat Foxp3 Staining Set, eBioscience, USA).

Table 2.4 – Flow cytometry antibodies used in the study with the respective conjugate, work dilution and distributor.

Antibody anti-mouse	Conjugate	Dilution	Distributor
anti-CD3 _ε	APC	1/100	eBioscience
anti-CD3 _{γδ}	PE	1/100	eBioscience
anti-B220	FITC	1/400	eBioscience
anti-B220	PE	1/800	eBioscience
anti-IgM	APC	1/250	eBioscience
anti-IgD	FITC	1/500	eBioscience
anti-CD5	PECy7	1/5000	eBioscience
anti-CD11b	PE	1/500	eBioscience
anti-B220	Pacific Blue	1/800	BioLegend
anti-CD25	APC	1/100	eBioscience

anti-CD4	FITC	1/400	eBioscience
anti-CD4	APC	1/400	eBioscience
anti-Foxp3	PE	1/100	eBioscience
anti-NK1.1	PE	1/100	eBioscience
anti-CD21	FITC	1/200	eBioscience
anti-CD23	PE	1/400	eBioscience

2.4.2. Effect of rshCD5 and rshCD6 injection in mice

To confirm that the results obtained in the characterization of lymphocyte populations were not due to artifacts of random transgenesis of the rshCD5 gene in transgenic mice, 25µg of exogenous rshCD5 were administered by i.p. injection to C57BL/6 WT mice for 15 days, on alternate days.

On the other hand, it was also conducted assays where 25µg of rshCD6 was injected to C57BL/6 WT mice for 15 days, on alternate days. Thus, it was possible to assess whether these two homologous molecules induce the same changes in the lymphocyte populations.

For this analysis the samples preparation protocol was the same as described above.

2.5. Immunization with T-independent type 1 and 2 and T-dependent antigens

To study the antibody response to TD and TI antigens, rshCD5tg mice and non-transgenic mice were immunized i.p. with 50µg TNP₅-KLH (as an example of TD), TNP_{0.3}-LPS antigen (TI-1) and TNP₆₅-Ficoll antigen (TI-2) in 200µL of PBS. TNP haptens conjugated with different antigens were supplied by Biosearch Technologies, Inc. USA. Serum from immunized mice were collected at days 0, 7, 14 (to TI response) and 21 (to TD response) after the primary immunization and stored at -20 ° C until analysis. Levels of TNP-specific antibodies were determined by ELISA. Briefly, plates were sensitized overnight with 3µg/mL TNP₁₈-BSA (Biosearch Technologies, Inc. USA) diluted in PBS, washed with PBS 0,05% Tween 20 and blocked with PBS 2% BSA for 1 h at 37°C. After doing a titration curve of serum for each antibody to select the best dilution, 100µL of antibody at the optimized dilution were added to the plate and incubated for one hour at RT (see table 2.5). To determine the levels of different isotypes of TNP-specific antibodies in the serum of immunized mice, biotinylated sheep anti-IgM, IgG1, IgG2a, IgG2b, IgG2c and IgG3 mouse (Jackson ImmunoResearch Laboratories, USA) were incubated for one hour at RT (see table 2.5). After three washes, Streptavidin-POD Conjugate (Roche Diagnostics) was added for 30min at RT. The assay was developed with 100µL of TMB (Tetramethylbenzidine, BD Biosciences, USA) for 30 min at RT in the dark. The reaction was stopped by adding 100µL of 2N sulfuric acid to each well. Subsequently the absorbance was measured in an ELISA reader (Gen5 1.09, Epoch, BioTek) at a wavelength of 450nm.

Besides the ELISA analysis some lymphocyte populations were also evaluated in spleen and peritoneal cavity by flow cytometry. The protocol followed was the same as mentioned above.

Table 2.5 – Table of anti-Immunoglobulin antibodies used and their working dilutions for each experiment type.

* α -mouse Ig	Ab dilution	Serum dilution TD	Serum dilution T.I. 1	Serum dilution T.I. 2
IgM	1/1250	1/500	1/500	1/1000
IgG1	1/10000	1/10000	1/500	1/1000
IgG2b	1/10000	1/10000	1/500	1/1000
IgG2c	1/10000	1/1000	1/500	1/1000
IgG3	1/10000	1/4000	1/500	1/1000

2.6. Experimental Tumor Models

The cell lines used in the experiments mentioned below were provided by the laboratory and all the cell lines used derived from murine cell lines. A stock of them was made for the assays performed. Those stocks were kept at -80°C in FCS inactivated – 10% DMSO. In the process of defrost was rapidly added culture medium to the cells in the cryotube in order to dilute the DMSO in contact with them. Then it was centrifuge 5min. at 1000rpm and resuspended in the appropriate culture medium and conditions (described below).

After the cells reached confluence, they were trypsinized with a 1x trypsin solution in PBS for 2min at 37°C . To finish take off them medium was added and then centrifuged and counted.

2.6.1. B16 melanoma cell line

For the study of melanoma tumors, the B16 melanoma tumor line was used. It is a non-lymphoid solid tumor that arises spontaneously in C57BL/6 mice. Cells were grown in DMEM media (Invitrogen, USA) supplemented with 10% FCS and 100IU/ml penicillin/streptomycin in a 5% CO_2 atmosphere. Different experimental tests have been conducted with this cell line and will be described below.

- **Subcutaneous injection:**

To evaluate the differences in tumor growth between the rshCD5Tg (n=15) and non-transgenic mice (n=8), after optimizing the appropriate cell number, 1×10^5 B16 cells were injected s.c. on the dorso of mice anesthetized with Isoflurane using a 23G needle. Every two days the tumor growth *in vivo* was checked and its diameter measured with a Vernier calliper (Sigma-Aldrich, Scienceware, USA). Upon reaching a certain size the mouse was euthanized with Isoflurane and the tumors extracted and conserved at -80°C for further studies (Cytokines Analysis) or placed in a fixative solution (PBS-4% PFA, EMSDiasum, USA) for 24 hours for further histological studies.

- **Intravenous injection:**

For experimental metastasis assays (n=16), 1×10^5 B16 cells were injected i.v. in the tail vein of mice anesthetized with Isoflurane. After 15 days, mice were euthanized with Isoflurane, their lungs were removed and the number of metastasis that appeared on the surface of the lung counted by two independent observers.

- **Effect of rshCD5 and rshCD6 as an adjuvant to chemotherapy:**

To study the effect of rshCD5 in the treatment of tumors with chemotherapy, two groups (n=5) of C57Bl/6 WT mice were analyzed. Group 1 mice were injected s.c. at day 0 with 1×10^5 B16 cells and, starting this day until the end of the experiment, injected i.p. with 25 μ g of rshCD5 (PX'Therapeutics, France) per mice every 48h. On the third day they also received a single dose of chemotherapy (Vincristine 1mg/kg (Pfizer, USA), Doxorubicin 3.3mg/kg (Pfizer, USA)). Group 2 was treated equally but instead of the rshCD5 treatment they received the same volume of PBS. The tumor growth was measured in both groups up to day 20, when all the mice were euthanized.

The same protocol was followed to study the effect of rshCD6 as a chemotherapy adjuvant, injecting 25 μ g of rshCD6 instead of rshCD5. In this case the tumor growth was monitored until day 18, when all the mice were euthanized.

2.6.2. RMA-S lymphoma cell line

To verify that the response observed was not specific of the melanoma cell line B16, other tumor models were evaluated, such as the lymphoma cell line RMA-S. These cells were grown in RPMI 1640 (Lonza, Switzerland) supplemented with 10mM HEPES, 2mM Glutamine, 10% FCS, 1mM sodium pyruvate and 100 IU/ml penicillin/streptomycin. To optimize the number of cells to be injected, two concentrations were tested. One group (n=5) of anesthetized C57BL/6 mice was injected s.c. on the dorso with 2×10^5 RMA-S cells, and the other (n=4) with 5×10^5 RMA-S cells using a 23G needle. Every two days the tumor growth *in vivo* was checked and its diameter measured with a Vernier calliper. Upon reaching a certain size the mouse was euthanized with Isoflurane.

2.6.3. MCA 205 sarcoma cell line

The other tumor model evaluated was the sarcoma cell line MCA 205. These cells were grown in RPMI 1640 (Lonza, Switzerland) supplemented with 2mM Glutamine, 10% FCS, 1mM sodium pyruvate, 10mM Hepes and 100IU/ml penicillin/streptomycin at 37°C, 5%CO₂ atmosphere. As a first attempt to optimize the number of cells to inject, rshCD5tg and non-transgenic anesthetized mice (n=5 for each group) were injected s.c. on the dorso with 1×10^6 MCA cells using a 23G needle. Every

two days the tumor growth *in vivo* was checked and its diameter measured with a Vernier calliper. Upon reaching a certain size the mouse was euthanized with Isoflurane and the tumors extracted and conserved at -80°C for further studies (Cytokines Analysis) or placed in a fixative solution (PBS-4% PFA) for further histological histology studies.

2.6.4 Measurement of cytokines levels in tumor extracts by ELISA

As described before, some tumor samples were preserved at -80 °C in order to analyze their cytokine profile. The protocol used was based on Matalka *et al.*, 2005. Murine IL-1 β , IL-6, IL-10 and TNF α were analyzed for each sample. The tumors were homogenized with a tissue disrupter (1mL Dounce Tissue Grinder, Wheaton, USA) in a solution of PBS-0.1% NP40 plus 1x protease inhibitors (Complete, Roche), then centrifuged at 5000 rpm for 15min at 4 °C. 100 μ L of undiluted sample were analyzed according to the manufacturer's instructions (Mouse ELISA Set, BD OptEIA, BD Bioscience).

2.6.5. AOM/DSS colon carcinogenesis murine model

A model of cancer of inflammatory origin was also studied, the AOM/DSS model (adapted from Suzuki *et al.*, 2006). Both rshCD5Tg and non-transgenic mice were injected with 20mg/Kg or 10mg/Kg of Azoxymethane (Sigma-Aldrich, USA) in PBS. A week later, the mice's drinking water was changed to a solution of 3% DSS (MP Biomedicals, LLC, France) in tap water for four days. Two weeks later, the water was again changed to 3% DSS in water for another 4 days. Ten weeks later the mice were euthanized with Isoflurane and their colons excised, flushed with PBS, cut longitudinally and fixed in PBS-4% PFA to further histological studies.

2.7. Data Analysis

For this study the graphs and statistical analysis were performed in GraphPad Prism 5.03. To compare the different groups studied the unpaired t-student test was used.

The standard curves in Microsoft® Office Excel®.

The analysis of the results obtained by the FACS Canto I flow cytometer was performed in FlowJo v5.7.2.

3. Results

3.1. Genotyping of mice

The aim of this study was to further the knowledge of the immunomodulating properties of CD5 and CD6. For these studies, a colony of rshCD5 transgenic mice was generated and maintained. This colony was reviewed once a week and three different breeding crosses made. Once new born mice reached the age of 4 weeks, they were weaned and genotyped by taking a DNA sample from an ear punch. PCR reactions were then carried out, which made possible to determine which mice were transgenic for the rshCD5 gene or non-transgenic by the presence or absence of a 450Kb fragment, respectively (Fig. 3.1). This fragment corresponds to the transgene, as it is amplified by primers specific for the extracellular region of human CD5, inserted into the mice genome. The 150Kb fragment also present in the image corresponds to the internal PCR control, the amplification of the LIEX gene (region of the invariant chain Li of MHC class I), present in all C57BL/6 mice. In Fig. 3.1 **A.**, besides the negative control, all samples are positive, so all mice are rshCD5 transgenic. This was expected because they originate from the crossing of a rshCD5 homozygote male and a transgenic female (homozygote or heterozygote). In Fig. 3.1 **B.**, some samples are positive (1.1, 1.3, 1.4, 15.5, 15.7) and others are negative (1.2, 15.4, 15.6, 15.8, 15.9), as the offspring analyzed comes from the breeding of a rshCD5 heterozygote male and a C57BL/6 WT female. In Fig. 3.1 **C.**, all the samples are positive again, as it can be seen, because the offspring analyzed comes from the crossing of a rshCD5 homozygote male and a C57BL/6 WT female.

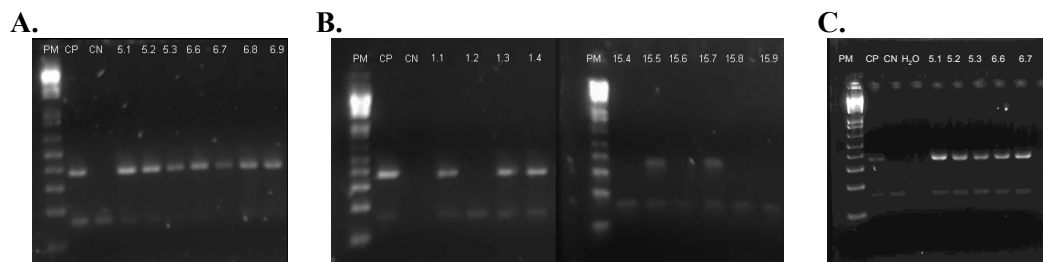


Fig. 3.1 – Illustration of agarose electrophoresis gels obtained from the DNA screening of rshCD5 transgenic and non-transgenic mice by PCR. The presence of the gene originates a fragment of 450bp and the internal control (Li gene) generates a band of 150bp. The PCR products were separated on a 2% agarose gel containing a 10,000x dilution of SYBR Safe and visualized in a G:Box appliance. **A.** Offspring of a cross between a homozygote male and a transgenic female (5.1/5.2/5.3 – males and 6.6/6.7/6.8/6.9 – females). **B.** Offspring of a cross between a heterozygote male and a C57BL/6 WT female (1.1/1.2/1.3/1.4 – females and 15.4/15.5/15.6/15.7/15.8/15.9 – males). **C.** Offspring of a cross between a homozygote male and a C57BL/6 WT female. (5.1/5.2/5.3 – males and 6.6/6.7 – females). PM – molecular weight, CP – Positive control, CN – Negative control.

3.2. Validation of the results with transgenic mice injecting rshCD5 in wild-type mice

To confirm that the results obtained in the characterization of the transgenic mice were not due to artifacts of random insertion of the rshCD5 gene, exogenous rshCD5 was administered by i.p. injection to C57BL/6 WT mice. Before use, the biological functionality of the commercial rshCD5 was checked with some experiments.

3.2.1. Confirmation of biological functionality of commercial lots of rshCD5 by ELISA

It has already been shown that rshCD5 binds to conserved components of the fungal cell wall (Vera *et al.*, 2008), so this interaction was verified by ELISA. Before the assay was started, rshCD5 and BSA (negative control to the ELISA) were biotinylated. A Western Blot analysis confirming the biotinylation can be seen in Fig. 3.2, where HSAb is the positive control. The observed molecular weights are the expected for all the samples: rshCD5 – 57KDa, BSA and HSA – approximately 66KDa.

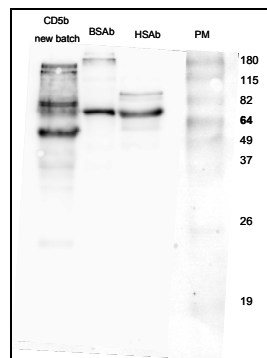


Fig. 3.2 – Western Blot confirming the biotinylation of a new batch of rshCD5 and BSA. The biotinylated proteins were separated by SDS-PAGE electrophoresis and analyzed by Western blotting. The Western blot was developed with streptavidin-HRP. From the left, samples include new rshCD5 batch (CD5b new batch), bovine serum albumin (BSAb) and human serum albumin (HSA). Molecular weight markers (PM) are shown in the first lane on the right.

As the extracellular domain of CD5 binds directly to components of the fungal cell wall, an ELISA plate was coated with zimosan (Zym), β -D-Glucan and Mannan. Increasing amounts of protein (rshCD5b or BSAb) were incubated and developed with streptavidin-HRP. In Fig. 3.3, it is possible to see that both rshCD5 (the already checked lot and the new) bind to Zym. rshCD5 also binds to β -D-Glucan, albeit with less affinity, and even less to Mannan. The differences of signal intensity observed between the new and the checked lot can be caused by differences in the biotinylation process (a random number of biotin molecules binds to each protein molecule).

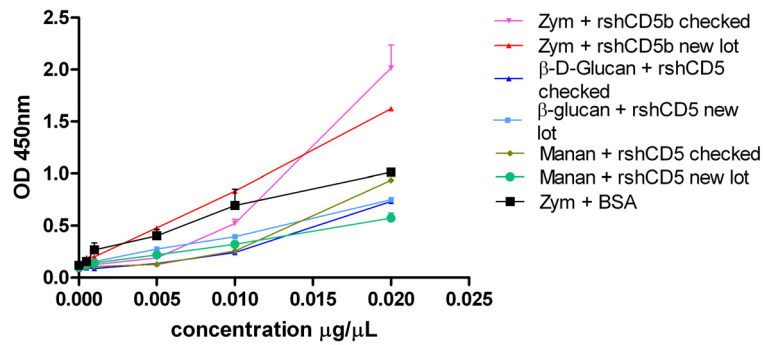


Fig. 3.3 – rshCD5 binding to different yeast wall components. ELISA plates coated with zymosan (ZYM), β -D-glucan and mannan were incubated with increasing amounts (0,05–2 μ g) of biotinylated rshCD5. Bound protein was detected with HRP-streptavidin (SAv).

3.2.2. Confirmation of new lot functionality by a sepsis model

Once the rshCD5 was checked *in vitro*, an *in vivo* assay was also performed. This experiment is based on the protective role of rshCD5 in Zym-induced septic shock. rshCD5 can interact with Zym and could therefore block its interaction with cell receptors, reducing Zym-induced cell signaling. After a single i.p. dose of rshCD5 (or BSA), a dose of Zym was injected into CD1 or C57BL/6 WT mice. Fig. 3.4 shows that 18h after the Zym challenge, the CD1 mice pretreated with rshCD5 show a better clinical score than the BSA-pretreated mice.

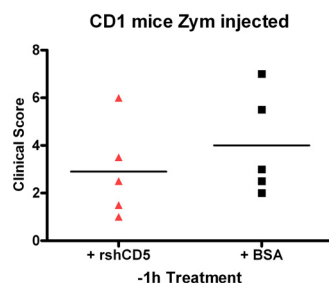


Fig. 3.4 – CD1 mice sensitivity to septic shock induced by zymosan. Septic shock was induced in CD1 mice of 7-9 weeks of age by i.p. administration of ZYM (500mg/kg) after pretreatment with BSA or rshCD5 (25 μ g, i.p.) 1 h before infusion of zymosan. 18 hours after injection the individual clinical scores were determined (0 - no symptom, 1 - weak symptoms, 2 - moderate symptom, 3 - severe symptoms; septic shock parameters: lethargy, diarrhea, conjunctivitis and hackles). The bar represents the average of the values from each group (n = 5).

At this time, 18h after the Zym challenge, the mice were sacrificed and serum samples collected. The levels of IL-6, an anti-inflammatory cytokine, were analyzed by ELISA (Fig. 3.5). Unexpectedly, the mice pretreated with rshCD5 showed higher levels of IL-6 than BSA-pretreated mice, which does not tie in well with the better clinical score displayed by these mice.

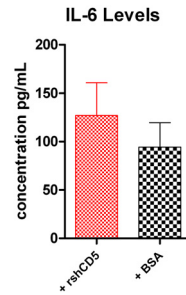


Fig. 3.5 – Inflammatory response 18h after induction of septic shock by zymosan. Septic shock was induced in CD1 mice of 7-9 weeks of age by i.p. administration of ZYM (500mg/kg) to mice pretreated with BSA or rshCD5 (25 µg, i.p.) 1 h before infusion of zymosan. 18 hours after induction of the septic shock the levels of inflammatory cytokines (IL-6) in the serum of mice were analyzed by ELISA. Data are presented as mean \pm SD (n = 5).

When the C57BL/6 mice were studied, both groups (rshCD5 and BSA pretreatment) revealed a worse clinical score compared to CD1 mice. However, the rshCD5 group still showed a lower clinical score than the BSA group (Fig. 3.6).

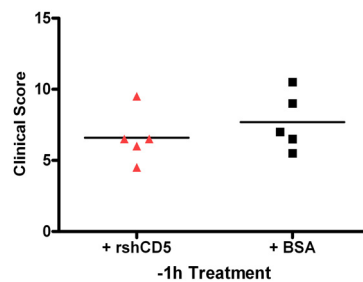


Fig. 3.6 – C57BL/6 WT mice sensitivity to septic shock induced by zymosan. Septic shock was induced in C57BL/6 WT mice of 7-9 weeks of age by i.p. administration of ZYM (500mg/kg) to mice pretreated with BSA or rshCD5 (25 µg, i.p.) 1 h before infusion of zymosan. 18 hours after injection the individual clinical scores were determined (0 - no symptom, 1 - weak symptoms, 2 - moderate symptom, 3 - severe symptoms; septic shock parameters: lethargy, diarrhea, conjunctivitis and hackles). The bar represents the average of the values of each group (n = 5).

The analysis of inflammatory cytokine levels (Fig. 3.7) showed that the rshCD5 group has lower levels of IL-6 and IL-1 β than the BSA group.

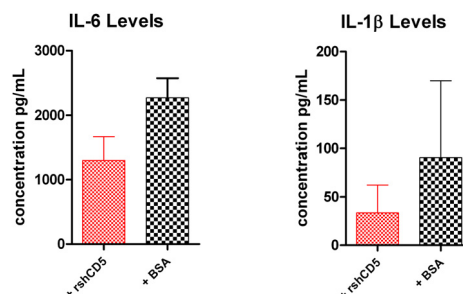


Fig. 3.7 – Inflammatory response 18h after induction of zymosan septic shock by zymosan. Septic shock was induced in C57BL/6 WT mice of 7-9 weeks of age by i.p. administration of ZYM (500mg/kg) to mice pretreated with BSA or rshCD5 (25 µg, i.p.) 1 h before infusion of zymosan. 18 hours after induction of the septic shock the levels of inflammatory cytokines (IL-6 and IL-1 β) in the serum of mice were analyzed by ELISA. Data are presented as means \pm SD (n = 5).

3.2.3 Detection of serum levels by ELISA after rshCD5 injection

To better understand the effect of rshCD5 on clinical scores and cytokine levels, the levels of this protein after infusion were measured in mouse serum. A single rshCD5 dose was administered and serum samples collected at different times. The serum levels of rshCD5 were then detected with a sandwich ELISA. In Fig. 3.8 **A.** the standard curve performed with known concentrations of commercial rshCD5 is represented, while Fig. 3.8 **B.** shows the concentrations of rshCD5 detected in serum samples. There appears to be a peak at 1h post administration, which decreases over time until reaching the basal levels at 6h post injection.

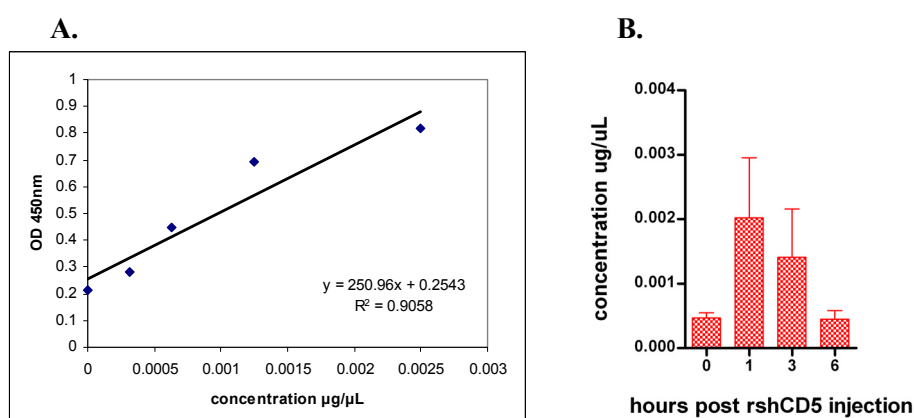


Fig. 3.8 – Detection of exogenously administrated rshCD5 in C57BL/6 WT mice. **A.** Standard curve performed with commercial rshCD5. **B.** Concentration of rshCD5 in C57BL/6 WT mice serum samples at different times post injection. Data are presented as mean \pm SD (n = 3).

3.3. Characterization of lymphocyte populations in mice

3.3.1. rshCD5 transgenic mouse

To further the characterization of the transgenic mice generated in the laboratory, more cellular populations were analyzed.

One of the populations analyzed in rshCD5Tg and non-transgenic mice was the $\gamma\delta$ T lymphocytes, which are related to tumor development. After the cells were stained, they were analyzed by flow cytometry. Firstly, the lymphocyte population was gated (Fig. 3.9 **A.**) and then the non-B lymphocytes (B220⁻), in other words the T lymphocytes, were selected for further analysis (Fig. 3.9 **B.**). Then the $\gamma\delta$ T lymphocytes were detected as CD3 $\gamma\delta$ ⁺CD3 ϵ ⁻ (Fig. 3.9 **C.**).

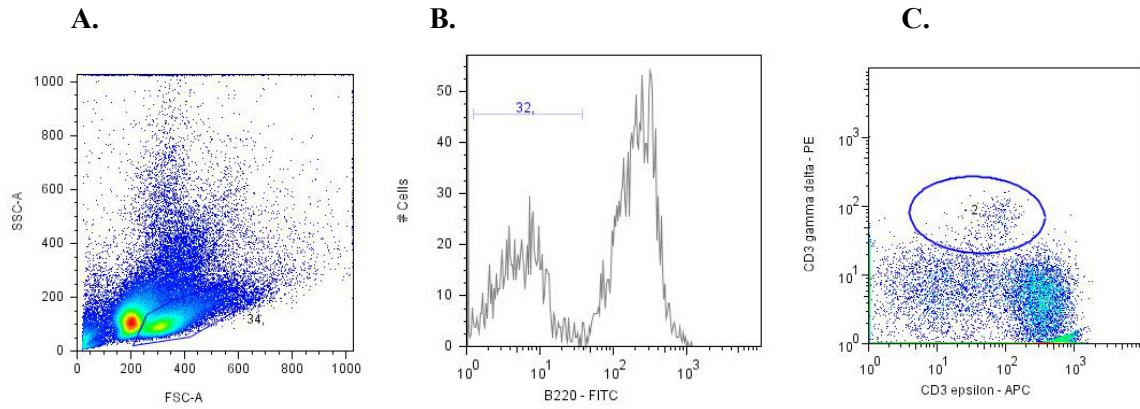


Fig. 3.9 – Flow cytometry analysis of $\gamma\delta$ T cells in rshCD5Tg and non-transgenic mice. **A.** Dot plot showing lymphocyte gating. **B.** Histogram showing the FITC channel and the FITCB220 negative cells selected. **C.** Gating of $\gamma\delta$ T cells. Thymus and spleen cells were stained with Abs anti-CD3 $\gamma\delta$ and anti-CD3 ϵ to identify cells with a double negative (CD3 $\gamma\delta^-$ CD3 ϵ^-), double positive (CD3 $\gamma\delta^+$ CD3 ϵ^+), and single positive (CD3 $\gamma\delta^+$ CD3 ϵ^- or CD3 $\gamma\delta^-$ CD3 ϵ^+) phenotype.

The samples were collected from rshCD5Tg and non-transgenic mice thymus and spleen. It is possible to see a tendency for the transgenic mice to possess higher levels of this population than the non-transgenic mice (Fig. 3.10).

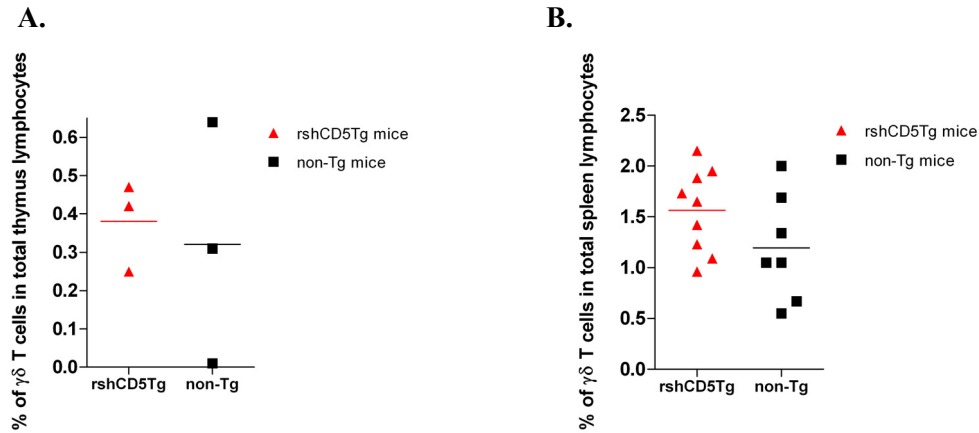


Fig. 3.10 – Percentage of $\gamma\delta$ T cells in lymphocytes. **A.** Percentage of $\gamma\delta$ T cells in thymus lymphocytes (n=3) in rshCD5Tg and non-transgenic mice. **B.** Percentage of $\gamma\delta$ T cells in spleen lymphocytes (n=8) in 7/10 week old rshCD5Tg and non-transgenic mice. The bars represent the average value for each group.

Another important cell population in the immune response is the Marginal Zone B cell population. These cells have a role in the T-independent cell response, also studied in this report (see section 3.5). The spleen lymphocytes were gated (Fig. 3.11 A.) and then the B lymphocytes – FITC B220 positive were selected for further analysis (Fig. 3.11 B.). From the gated B lymphocyte population, the MZ cells are characterized by the CD21^{high}CD23^{low} phenotype (gate in Fig. 3.11 C.).

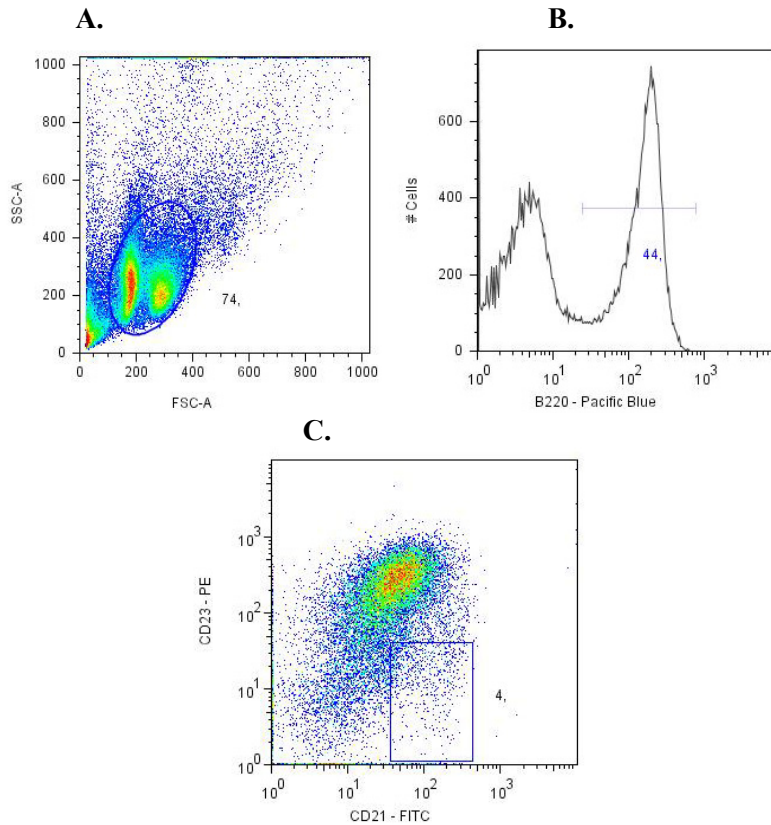


Fig. 3.11 – Flow cytometry analysis of MZ cells in rshCD5Tg and non-transgenic mice. **A.** Dot plot showing lymphocyte gating. **B.** Histogram showing the Pacific Blue channel and the Pacific Blue B220 positive cells selected. **C.** Gating of MZ cells. To identify MZ cells, the samples were stained with Abs anti-CD21 and anti-CD23. MZ cells are CD21^{high} CD23^{low}.

Fig. 3.12 shows that rshCD5Tg mice display a higher percentage of MZ cells than non-transgenic mice littermates.

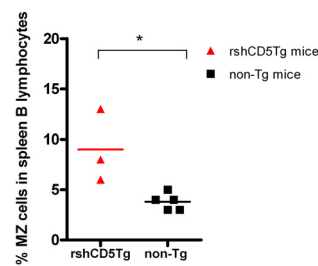


Fig. 3.12 – Percentage of MZ cells in spleen lymphocytes (n=5) in 7/10 week old rshCD5Tg and non-transgenic mice. The bars represent the average value for each group. The unpaired t-test was performed to compare the differences, * p<0,02.

The natural killer T cells (NKT – CD3⁺NK1.1⁺) are another population involved in the regulation of the immune system, and they express CD5 in their cellular membrane. Analysis of NKT cells was performed after gating the spleen lymphocytes (Fig. 3.13 A). With this approach, it is possible to analyze both NKT (APC CD3ε⁺ PE NK1.1⁺) and NK cells (APC CD3ε⁺ PE NK1.1⁺).

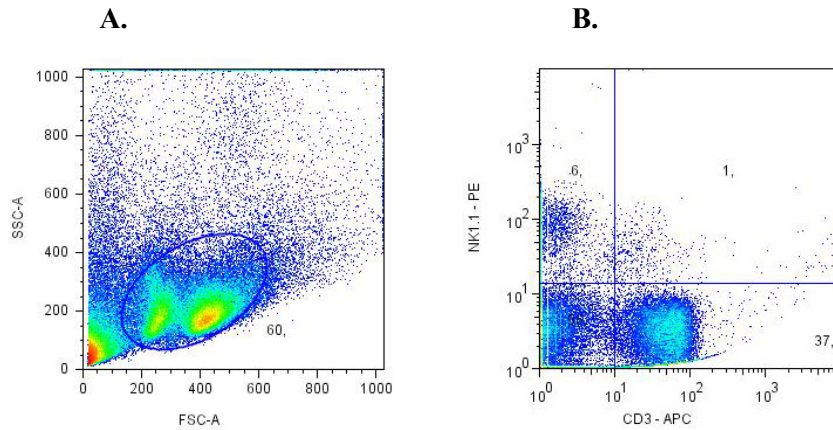


Fig. 3.13 – Flow cytometry analysis of NKT spleen cells in rshCD5Tg mice. **A.** Dot plot showing the gating of spleen lymphocytes. **B.** Dot plot showing the double negative, double positive and single positive populations. The samples were stained with Abs anti-NK1.1 and anti-CD3ε.

There are no apparent differences between rshCD5Tg and non-transgenic mice regarding NK cells, but transgenic mice display a higher percentage of NKT cells (Fig. 3.14).

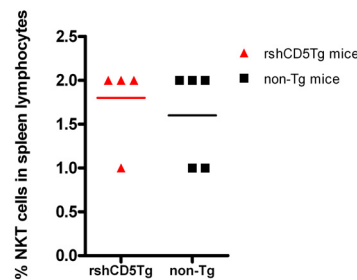


Fig. 3.14 – Percentage of NKT spleen cells in 7/10 week old rshCD5Tg and non-transgenic mice (n=5). The bars represent the average value for each group.

3.3.2. Effect of rshCD5 and rshCD6 injection in mice

To demonstrate that the presence of rshCD5 was responsible for the phenotype observed in the transgenic mice, exogenous rshCD5 was administered to C57BL/6 WT mice and the percentages of relevant cell populations analyzed.

It was observed that transgenic mice displayed lower levels of Treg cells than the non-transgenic mice. This population can play a key role in suppressing T-cell-mediated immunity in patients with cancer. To analyze this population, lymphocytes were gated according to size and granularity (Fig. 3.15 A.), and Treg cells detected as FITC CD4⁺ APC CD25⁺ (Fig. 3.15 B.) but also PE Foxp3⁺ (Fig. 3.15 C.).

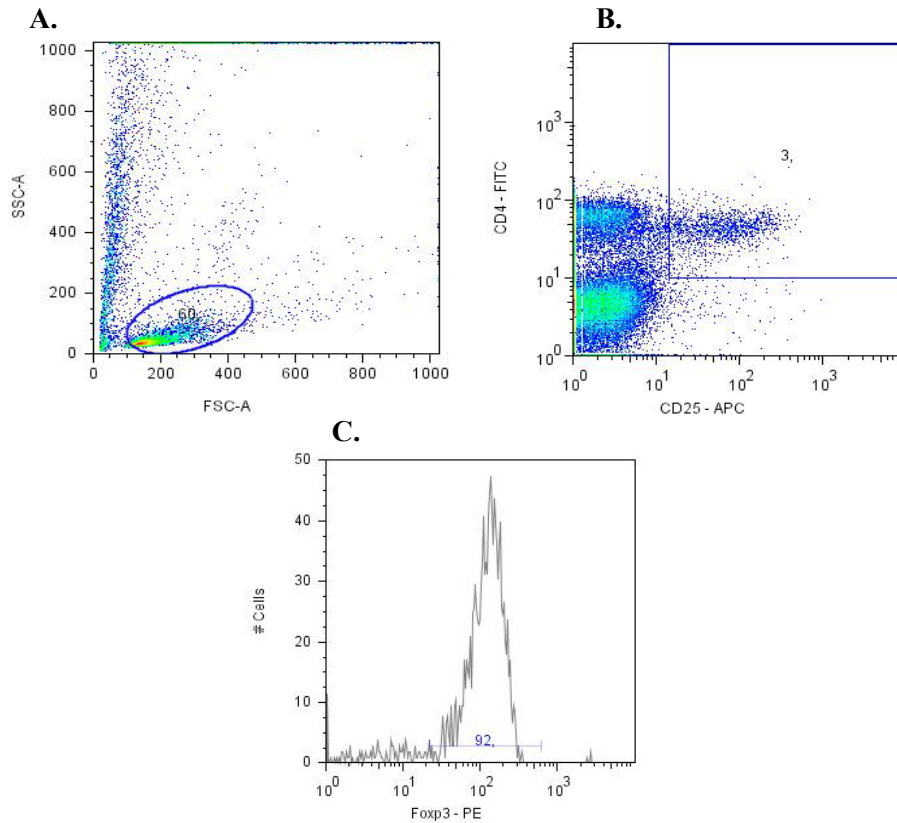


Fig. 3.15 – Flow cytometry analysis of peritoneal Treg cells. **A.** Dot plot showing the gating of lymphocytes. **B.** Dot plot representing a sample analyzed for CD4 and CD25 staining. The samples were stained with Abs anti-CD4, anti-CD25 and anti-Foxp3. **D.** Histogram of the double positive gate showing the percentage of the population in that gate expressing FoxP3.

The first assay performed was based on the administration of rshCD5, rshCD6 and BSA, respectively, i.p. to C57BL/6 WT mice for 15 days, on alternate days; a different scheme was also set up, where rshCD5 and BSA were administered every 12h for 15 days. Fig. 3.16 shows the analysis of relevant cell populations following the above mentioned treatments.

As shown in Fig. 3.16 **A.**, the percentage of peritoneal NK cells did not change significantly with either of the treatments, although a tendency towards a decrease in these cells can be observed in the group treated with rshCD6. In spleen NK cells (Fig. 3.16 **B.**), mice treated with rshCD5 every 48h appear to have a higher percentage of these cells; this also happens in rshCD5 mice treated every 12 h, although in this case the increase is non-significant.

Analysis of the peritoneal NKT population (Fig. 3.16 **C.**) revealed that treatment with rshCD6 results in a lower percentage of these cells as compared to the other two groups; no other significant changes were observed. However, in spleen (Fig. 3.16 **D.**), NKT cells appear to be increased following treatment with rshCD5, regardless of the treatment scheme.

The last population analyzed, the peritoneal Treg cells (Fig. 3.16 **E.**), show a tendency to lower percentages in both the rshCD5 and rshCD6 48h groups. Unexpectedly, analysis of this population in spleen (Fig. 3.16 **F.**) revealed a tendency to higher percentages of these cells in the rshCD6 48h group.

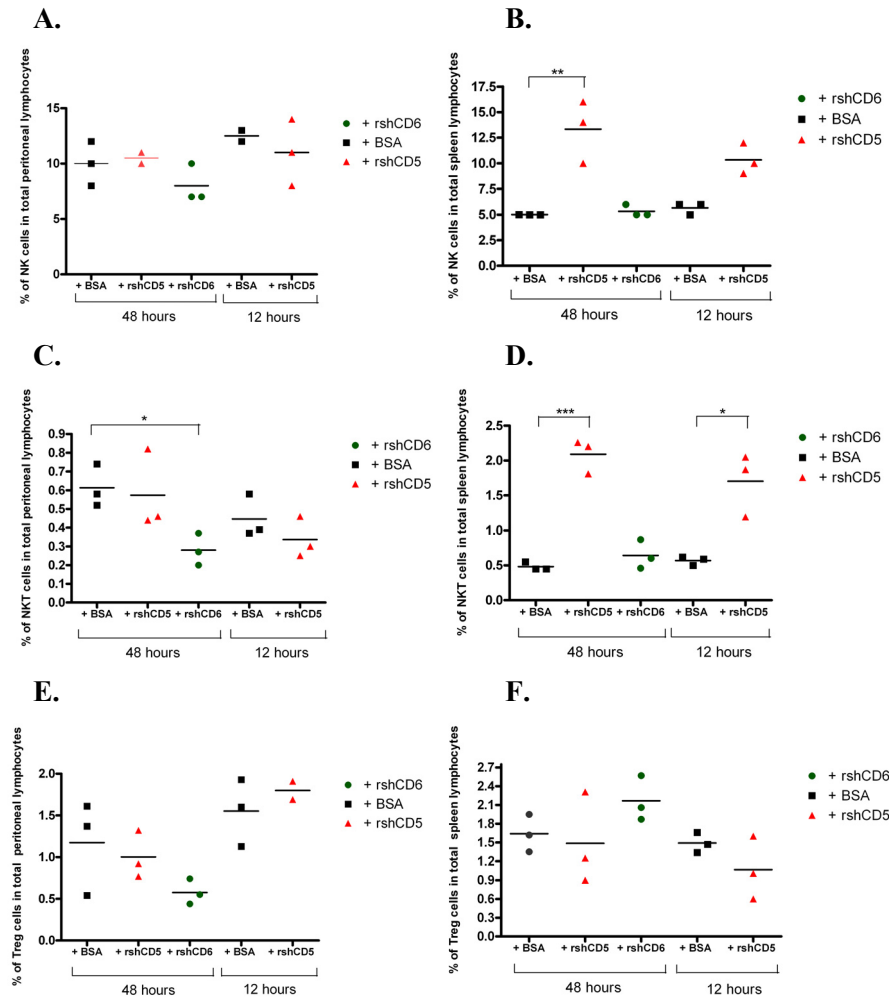


Fig. 3.16 – Percentage of peritoneal and spleen cell populations in 7/10 week old C57BL/6 WT mice (n=3). The first three groups were treated with 25 μ g of BSA, rshCD5 or rshCD6 i.p. for 15 days, on alternate days. The last two groups were treated with 6 μ g i.p. injection of BSA or rshCD5 for 15 days every 12h. **A and B.** Individual percentages of NK cells in total lymphocytes from the peritoneum and spleen, respectively. **C and D.** Individual percentages of NKT cells in total lymphocytes from the peritoneum and spleen, respectively. **E and F.** Individual percentages of Treg cells in total lymphocytes from the peritoneum and spleen, respectively. The bars represent the average value for each group. * $p < 0,02$, ** $p < 0,01$ and *** $p < 0,0005$.

To further the study of the effects of rshCD6 in immune cells, another subpopulation was analyzed, the B1 cells. For these assays, the injection protocol of choice was the treatment of C57BL/6 mice for 15 days, every other day. Control mice were treated with PBS.

B1 cells are APC IgM⁺ FITC IgD^{dull}, and can be gated as such from total lymphocytes (Fig. 3.17 **B.**). This population can be then divided into two sub-populations (Fig. 3.17 **C.**): the B1-a, PECy7 CD5⁺ Pacific Blue B220^{dull}, and B1-b, PECy7 CD5⁻ Pacific Blue B220⁺, cells.

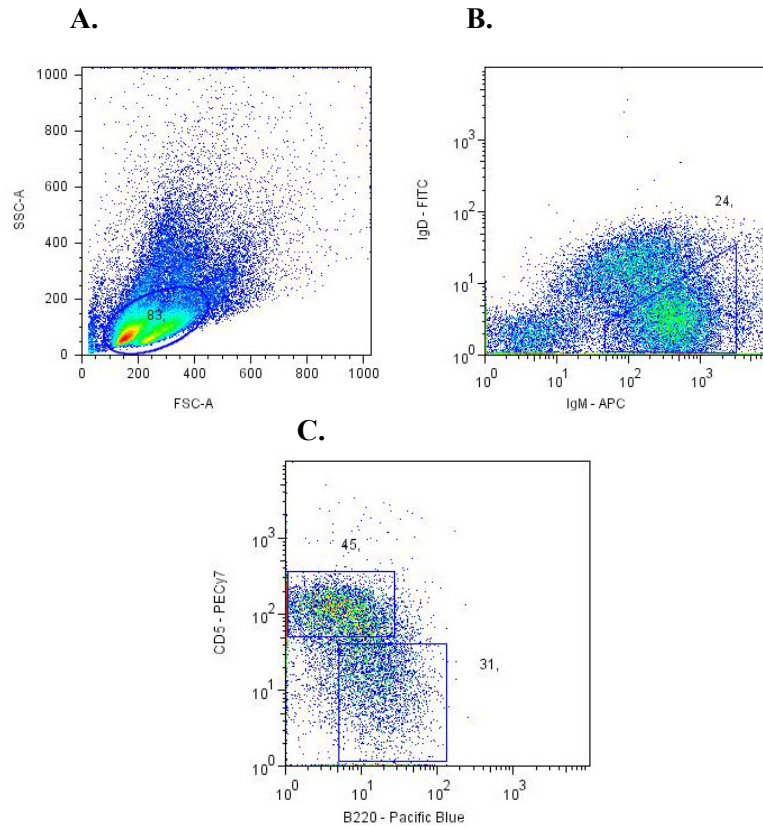


Fig. 3.17 –Flow cytometry analysis of peritoneal B-1 cells. **A.** Dot plot showing the gating of lymphocytes. **B.** Dot plot showing peritoneal cavity cells stained with antibodies against IgM and IgD. The relative expression of IgM and IgD can be used to discriminate $\text{IgM}^+\text{IgD}^{\text{dull}}$ B-1 cells (gate shown). **C.** Dot plot representing cells from the previous gate stained for the expression of B220 and CD5 to further distinguish $\text{CD5}^+\text{B220}^{\text{dull}}$ (B-1a cells) from $\text{CD5}^+\text{B220}^+$ (B-1b cells).

In this experiment it was possible to see that the peritoneal B1-a population is reduced, while the peritoneal B1-b population is increased in the group treated with rshCD6 as compared to the BSA group. In agreement with previous results, there were no differences in the spleen NKT population percentages, while spleen Treg cells showed a tendency to higher percentages.

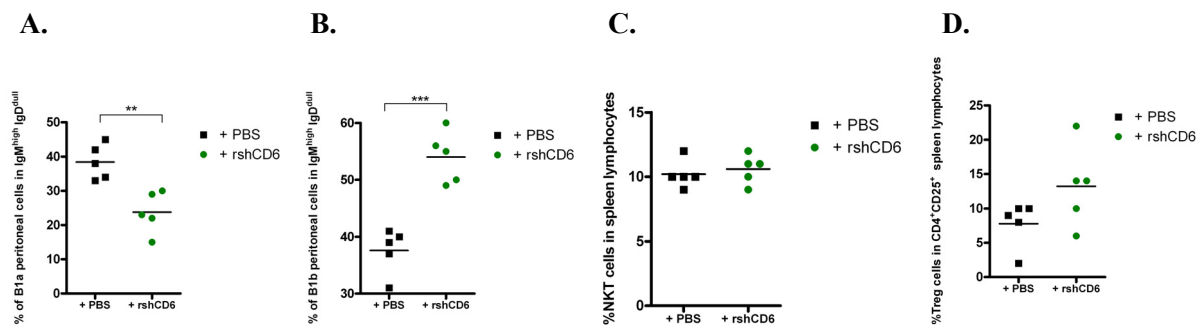


Fig. 3.18 – Percentages of cell subpopulations in treated and control mice. The groups (7/10 week old C57BL/6 WT mice (n=5)) were treated with 25 μg of rshCD6 or PBS i.p. for 15 days, on alternate days. **A.** Individual percentages of peritoneal B-1a cells. **B.** Individual percentages of peritoneal B-1b cells. **C.** Individual percentages of spleen NKT cells in total lymphocytes. **D.** Individual percentages of spleen Treg cells in spleen $\text{CD4}^+\text{CD25}^+$ cells. The bars represent the average value for each group. ** $p < 0,01$ and *** $p < 0,0005$.

3.4. Immunization with T-dependent and T-independent type 1 and 2 antigens

Characterization of rshCD5Tg mice revealed a reduction in some regulatory cell subpopulations (Treg and B10). This reduction might have an effect in the immune response, which makes it interesting to study the differences in response to T-dependent and T-independent stimuli between the rshCD5Tg and non-transgenic mice.

T-independent antigens are nonprotein Ag (polysaccharides, membrane glycolipids, nucleic acids) that induce humoral immune response (B lymphocytes) without the involvement of T cells as the helper T cells. This Ag stimulate Ab response without class switching, affinity maturation or memory B cell memory generation, helper T cells dependent processes. On the other hand, T-dependent antigens require activation of the T cells by Ag B cell presentation to them. Activated helper T cells stimulate the proliferation and differentiation of B cells and also affinity maturation, B cells memory generation and isotype switch, leading to the production of various Ig isotypes.

rshCD5Tg and non-transgenic mice were immunized i.p. with 50µg of TNP₅-KLH (T-dependent (TD) antigen) and the production of specific Abs to TNP₅ (IgM, IgG₁, IgG_{2b}, IgG_{2c}, IgG3) was measured in serum samples collected at different time-points post-immunization (Fig. 3.19). As shown in this figure, the levels of anti-TNP₅ IgM were higher in rshCD5tg mice at all time points analyzed. As for other immunoglobulins, at day 7 the rshCD5Tg mice show lower levels than non-transgenic mice, but at days 14 and 21 these become equal or even higher than in the non-transgenic mice.

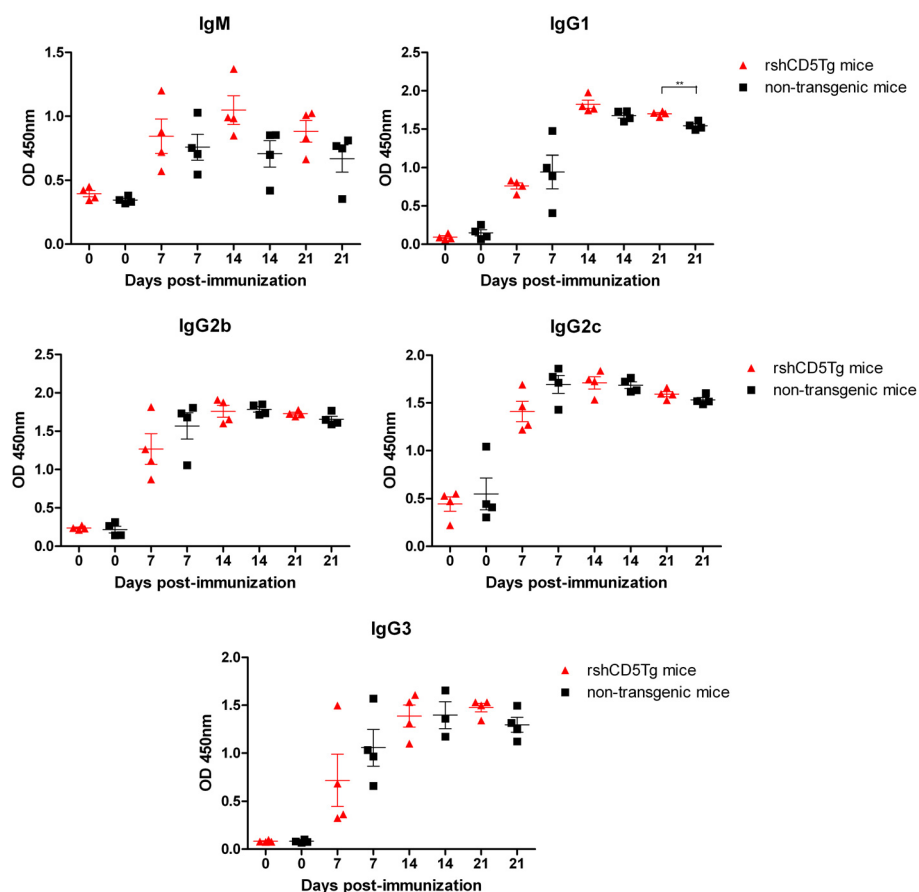


Fig. 3.19 – Hapten-specific antibody responses in rshCD5Tg and non-transgenic mice. The levels of specific immunoglobulins (Ig) against the hapten TNP were determined by ELISA in serum of rshCD5Tg (red triangles) and non-transgenic littermates (black squares) on day 0, 7, 14 and 21 after immunization with 50 μ g TNP₅-KLH (n = 4). Ig levels are expressed as OD 450 nm values. The bars represent the average value for each group. ** p<0,01.

At day 21, the mice were sacrificed and spleens were collected for subpopulation analysis. As shown in Fig. 3.20, both B1-a and B1-b subpopulations show a tendency for lower percentages in the rshCD5Tg mice compared to the non-transgenic mice.

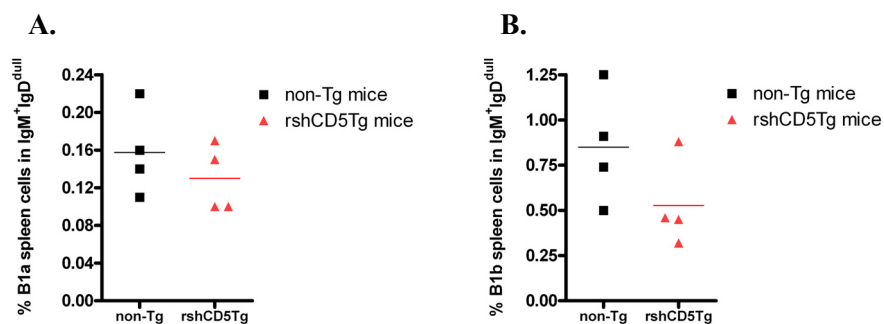


Fig. 3.20 – Percentage of spleen B-1 cells at day 21 post-immunization. The groups (7/10 week old rshCD5 and non-transgenic mice (n=4)) were immunized with 50 μ g TNP₅-KLH at day 0 and day 14. **A.** Individual percentages of spleen B-1a cells. **B.** Individual percentages of spleen B-1b cells. The bars represent the average value for each group.

The observed changes in the B1-a and MZ B cells populations (populations that produce Ab) in the rshCD5Tg mice, as well as the alterations in the T-dependent response in transgenic mice pointed to an enhanced immune response as a consequence of rshCD5 overexpression. It was then interesting to study whether there were also differences in T-independent (TI) responses, which would point to a generalized increase in the immune response in these mice. Once again rshCD5Tg and non-transgenic mice were immunized with 50 μ g of TNP_{0.3}-LPS (TI type 1) or TNP₆₅-Ficoll (TI type 2) i.p.. The specific anti-TNP Abs were detected in the serum samples collected at different times post-immunization (see Fig. 3.21 for TI type 1 and Fig. 3.22 for TI type 2).

It is possible to see in Fig. 3.21 that all the different immunoglobulin subtype levels in the rshCD5Tg mice are significantly higher than in the non-transgenic mice at day 7; at day 21 there are no statistically significant differences but it is possible to see a tendency.

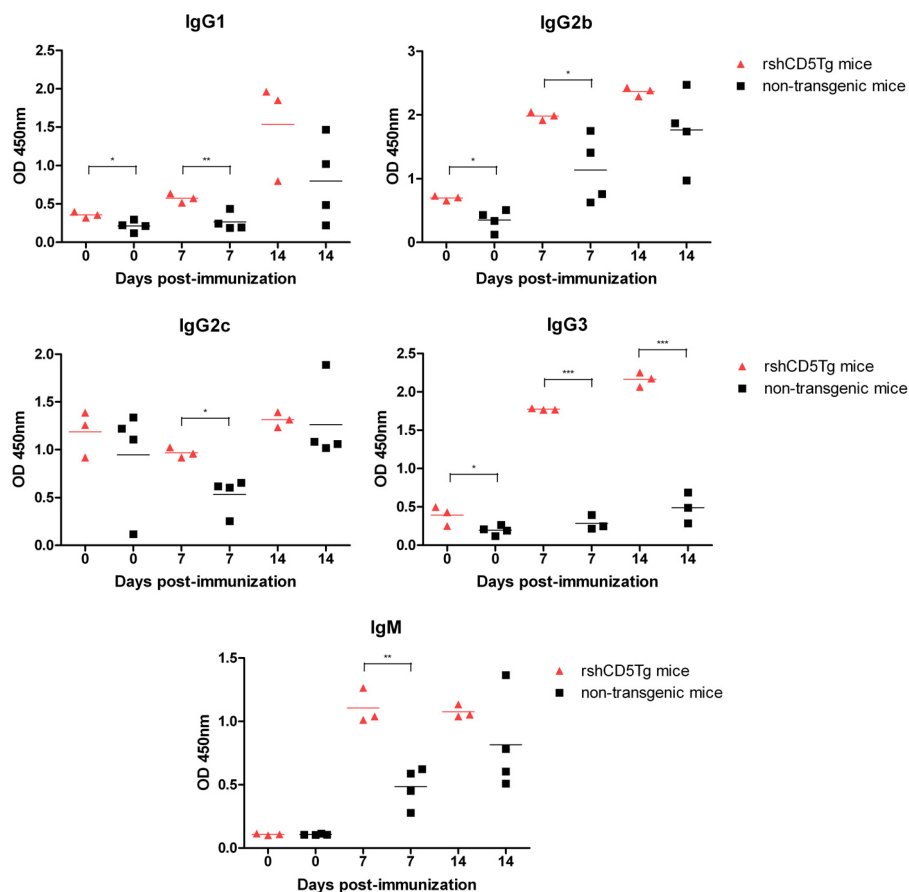


Fig. 3.21 –Hapten-specific antibody responses in rshCD5Tg and non-transgenic mice. The levels of specific immunoglobulins (Ig) against the hapten TNP TI-1 were determined by ELISA in serum of rshCD5Tg (red triangles) and non-transgenic littermates (black squares) (n = 4) on day 0, 7 and 14 after immunization with 50 μ g TNP_{0.3}-LPS. The 4 mice per group (n = 4) Ig levels are expressed as OD 450 nm values. The bars represent the average value for each group. * p<0,02, ** p<0,01 and ***p<0,0005.

However, no statistically significant differences in immunoglobulin levels were detected between rshCD5Tg and non-transgenic mice when analyzing their response to type 2 TI antigens.

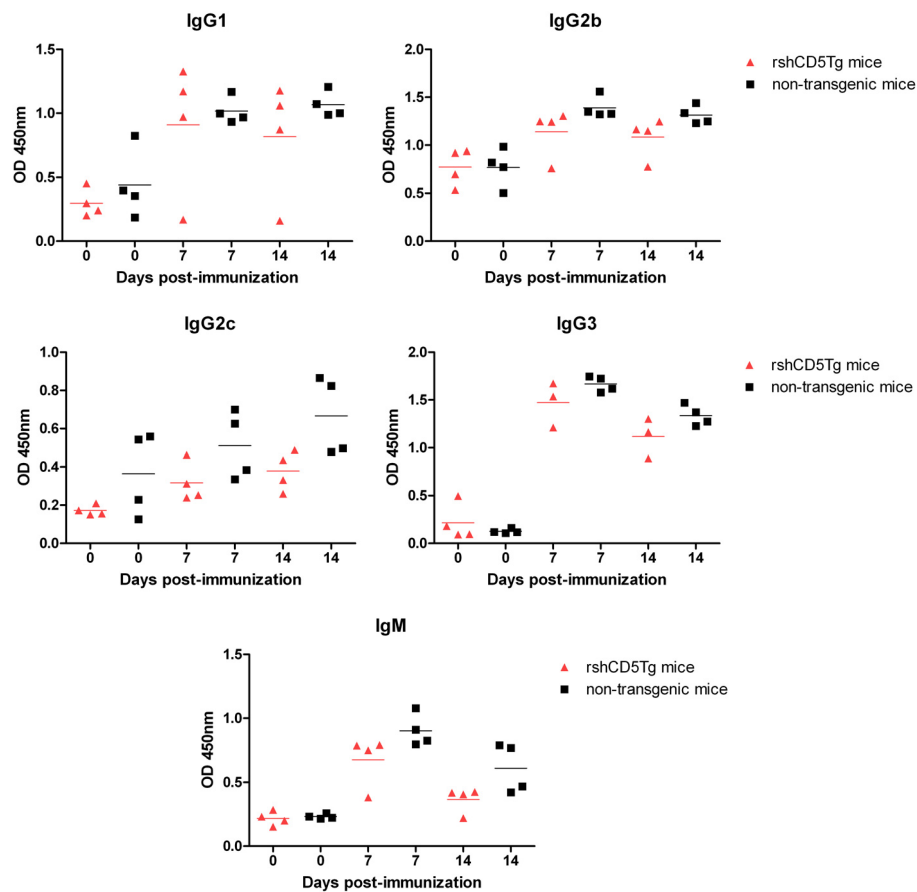


Fig. 3.22 – Haptenspecific antibody responses in rshCD5Tg and non-transgenic mice. The levels of specific immunoglobulins (Ig) against the hapten TNP TI-2 were determined by ELISA in serum of rshCD5Tg (red triangles) and non-transgenic littermates (black squares) ($n = 4$) on day 0, 7 and 14 after immunization with $50\mu\text{g}$ TNP₆₅-Ficoll. Ig levels are expressed as OD 450 nm values. The bars represent the average value for each group.

At day 14 all the mice (immunized with type 1 and type 2 TI antigens) were sacrificed and spleen and peritoneal lavage samples collected for further flow cytometry analysis of B1 subpopulations. Fig. 3.23 shows that the B1-a subpopulation shows a tendency to decrease following treatment with both TI antigens, type 1 and type 2. It can be seen in Fig. 3.23 C. that the spleen B1-b subpopulation does not experience changes in percentage in response to type 1 antigens, although rshCD5Tg mice show higher percentages of these cells in response to immunization with type 2 antigen. Peritoneal lavage samples show a higher percentage of B1-b cells in rshCD5Tg mice as compared to non-transgenic mice following immunization with type 1 antigen, although the opposite can be seen in mice immunized with type 2 antigen.

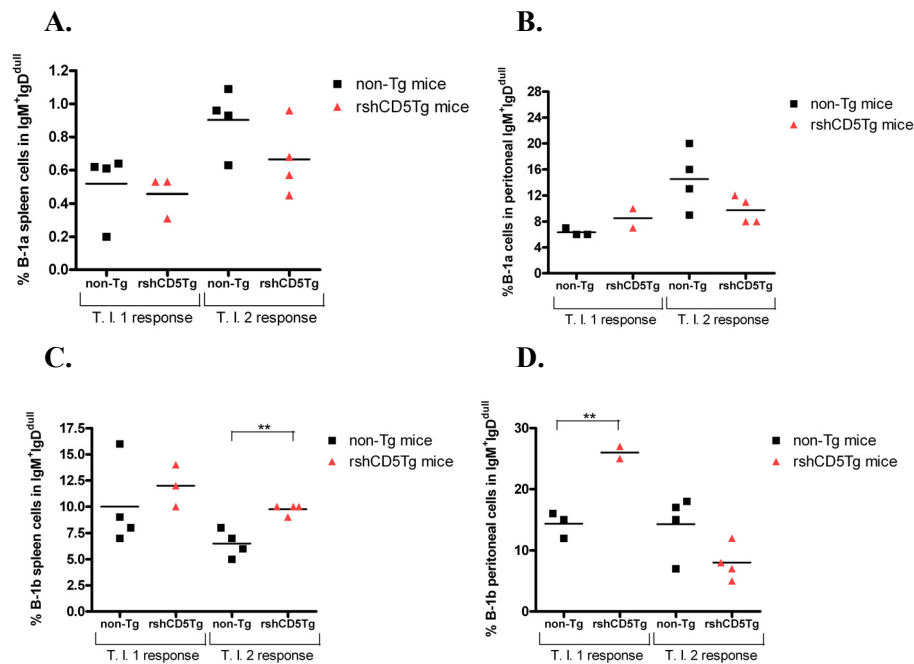


Fig. 3.23 – Percentage of spleen and peritoneal B-1 cells at day 14 post-immunization. The mice (n = 4, 7/10 week old rshCD5 and non-transgenic mice) were immunized with 50 μ g TNP_{0.3}-LPS (for TI type 1 response) and 50 μ g TNP₆₅-Ficoll (for TI type 2 response) at day 0. **A.** Individual percentages of spleen B-1a cells. **B.** Individual percentages of peritoneal B-1a cells. **C.** Individual percentages of spleen B-1b cells. **D.** Individual percentages of peritoneal B-1b cells. The bars represent the average value for each group. ** p<0,01.

These data suggest that rshCD5Tg mice present an increased response to both TD and TI antigen stimuli.

3.5. Experimental Tumor Models

To further the study of the role of the observed differences in regulatory cell subpopulations in rshCD5Tg mice, experimental tumor models were carried out in these mice. In this study, three different tumor models were used: melanoma, lymphoma and sarcoma models. A murine model of inflammatory carcinogenesis was also studied.

3.5.1. Role of rshCD5 in tumor development

3.5.1.1. B16 melanoma cell line

rshCD5Tg and non-transgenic mice were inoculated s.c. with 1×10^5 melanoma B16 cells and tumor size measured over 25 days. Fig. 3.24 **A.** represents the tumor diameter over time, with transgenic mice showing significantly slower growth of the subcutaneous tumor than the non-transgenic mice. Following this observation, an experimental metastasis assay was carried out to evaluate whether rshCD5Tg mice also show an advantage to metastatic spread. As shown in Fig. 3.24 **B.**, transgenic mice seem to have a lower number of pulmonary metastasis as compared to non-transgenic mice.

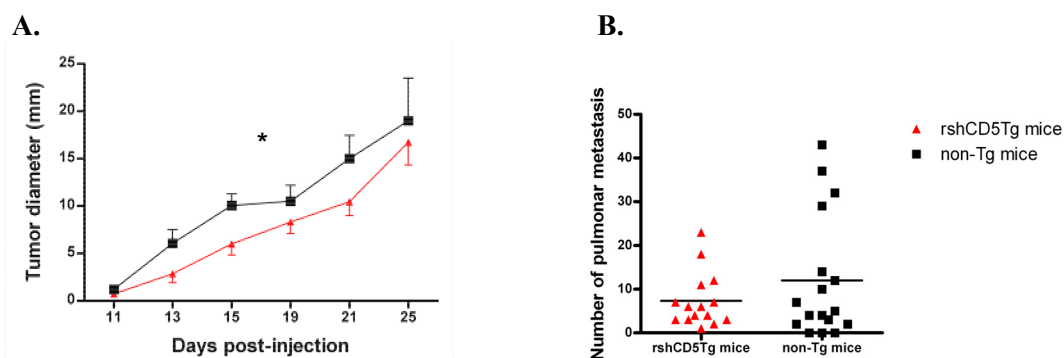


Fig. 3.24 – B16 tumor growth *in vivo*. **A.** 1×10^5 B16 cells were s.c. inoculated into rshCD5Tg (n=15) and non-transgenic littermates (n=8). The tumor was measured with a caliper over 25 days. Data are represented as mean \pm SD. * $p < 0,05$ **B.** Experimental metastasis assay. 1×10^5 B16 cells were inoculated i.v. in rshCD5Tg and non-transgenic littermates (n=16). Fifteen days later the mice were sacrificed, the lungs removed and the number of metastasis on the lung surface were macroscopically counted. The bars represent the average value for each group.

In this way, it could be said that the growth rate of B16 melanoma cells in rshCD5Tg mice is slower than in non-transgenic mice.

Another assay was carried out to study the effect of CD5 as an adjuvant of chemotherapy. For this experiment C57BL/6 mice were injected with CD5, or PBS as control, in chemotherapy-treated mice. Two groups of C57BL/6 WT mice were inoculated s.c. with 1×10^5 melanoma B16 cells and treated with rshCD5 or PBS every 48h throughout the assay. Three days after the B16 cells inoculation a single chemotherapy dose was administered. Tumor size was measured over 20 days. Fig. 3.25 represents the tumor diameter in the last day of the assay, and it can be easily seen that the mice treated with rshCD5 show a significantly slower diameter of the subcutaneous tumor than the mice treated with PBS.

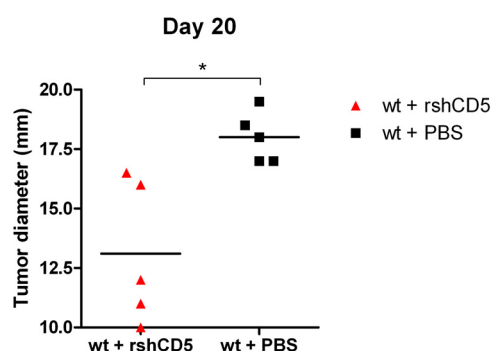


Fig. 3.25 – Effect of rshCD5 as a chemotherapy adjuvant. 1×10^5 B16 cells were s.c. inoculated into two groups of C57BL/6 WT mice (n=5). One group received a 25 μ g rshCD5 treatment (red) and the other the same volume of PBS (black). Three days post-tumor inoculation, both groups received a single dose of chemotherapy (Vincristine 1mg/kg and Doxorubicin 3.3mg/kg). The tumor was measured with a caliper. * $p < 0,02$

3.5.1.2. RMA-S lymphoma cell line

Another murine tumor model studied was the lymphoma model. As in the melanoma model, rshCD5Tg and non-transgenic mice were inoculated s.c. with RMA-S lymphoma cells. In this case it was necessary to optimize the number of cells inoculated and two doses were tried: 2×10^5 and 5×10^5 cells. Tumor size was measured over 21 days. Fig. 3.26 **A.** and **B.** shows the tumor diameter along the assay; it can be seen that at the higher cell concentration the transgenic mice have a tendency for a lower tumor growth rate than the non-transgenic mice. However, further studies will need to be carried out in this regard.

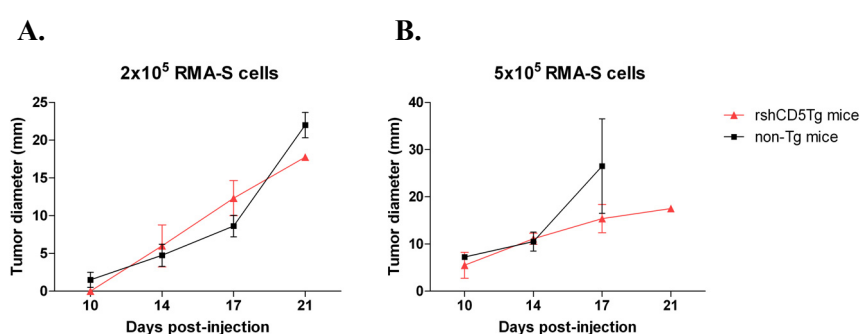


Fig. 3.26 – RMA-S tumor growth *in vivo*. **A.** 2×10^5 RMA-S cells were s.c. inoculated in rshCD5Tg and non-transgenic littermates mice (n=5). The tumor was measured over 21 days with a caliper. **B.** 5×10^5 RMA-S cells were s.c. inoculated in rshCD5Tg and non-transgenic littermates mice (n=4). The tumor was measured over 21 days with a caliper. Data are presented as mean \pm SD.

3.5.1.3. MCA 205 sarcoma cell line

The third murine tumor model studied was the sarcoma model. As in the other models, rshCD5Tg and non-transgenic mice were inoculated s.c. with 2×10^5 MCA 205 cells and tumor size measured over 15 days. Fig. 3.27 shows the tumor diameter throughout the assay, and it seems that the transgenic mice have a tendency to show a lower tumor growth rate than the non-transgenic mice. Further studies are needed in order to fully determine the effect of rshCD5 in MCA 205 tumor growth.

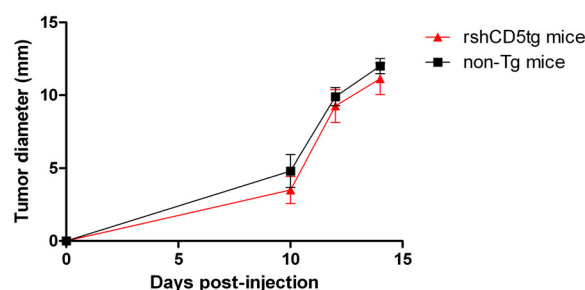


Fig. 3.27 – MCA 205 tumor growth *in vivo*. 2×10^5 MCA 205 cells were s.c. inoculated into rshCD5Tg and non-transgenic littermates (n=5). The tumor was measured for 15 days with a caliper. Data are presented as mean \pm SD.

3.5.1.4 Measurement of protein cytokines in tumor extracts by ELISA

At day 15 the mice inoculated with MCA 205 cells were sacrificed and the tumors extracted for further cytokine analysis. Murine IL-1 β , IL-6, IL-10 and TNF α (Fig. 3.28) were analyzed for each sample by ELISA in crude tumor extracts. The results were not statistically significant, but IL-6 levels showed a tendency to be higher in tumors from rshCD5Tg mice than from non-transgenic mice. Interestingly, IL-10 levels were slightly lower in rshCD5Tg than in non-transgenic mice.

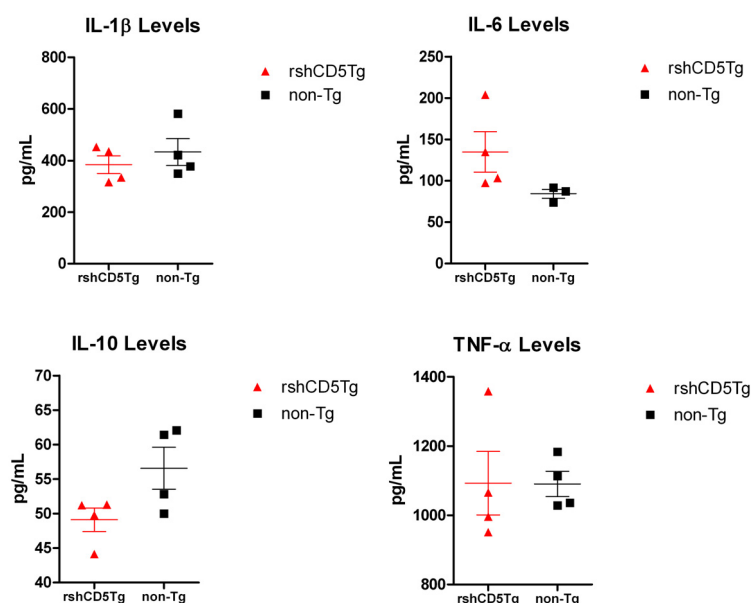


Fig. 3.28 –Murine IL-1 β , IL-6, IL-10 and TNF- α levels in tumor extracts by ELISA. The bars represent the average value for each group \pm SD (n = 4).

3.5.1.5. AOM/DSS colon carcinogenesis murine model

The last tumor model analyzed was a colon cancer of inflammatory origin model. This model was optimized with a very small number of animals, so the results cannot be statistically significant. However, it is possible to see a tendency for rshCD5Tg mice to show a lower number of tumors in their colon.

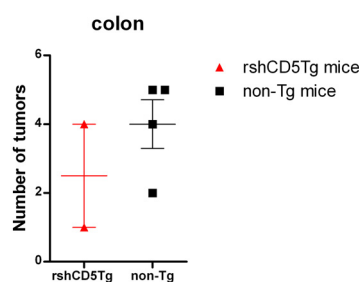


Fig. 3.29 – Number of colon tumors in mice treated with AOM/DSS. rshCD5Tg (n=2) and non-transgenic littermates (n=4) were injected with a single dose of AOM (20mg/kg i.p.) and then subjected to two cycles of 3% DSS in drinking water. Mice were sacrificed 12 weeks after AOM injection and their colons removed; macroscopical tumors were counted. The bars represent the average value for each group \pm SD.

3.5.2. Role of rshCD6 in tumor development

As previously mentioned, the CD6 molecule is highly homologous to CD5, so after the results obtained with rshCD5Tg mice and the mice treated with rshCD5 it was interesting to see whether CD6 could also improve the anti-tumor response. This assay was carried out by injecting C57BL/6 mice with CD6 or PBS as control, in chemotherapy-treated mice. The aim was to evaluate whether CD6 could be of use as an adjuvant to chemotherapy.

Two groups of C57BL/6 WT mice were inoculated s.c. with 1×10^5 melanoma B16 cells and treated with rshCD6 or PBS every 48h throughout the assay. Three days after the inoculation a single chemotherapy dose was administered. Tumor size was measured over 18 days. Fig. 3.30 represents the tumor diameter along the assay, and it can be easily seen that the mice treated with rshCD6 show a slower growth tendency, particularly in the first days, of the subcutaneous tumor than the mice treated with PBS. At day 18 post-tumor inoculation, administration of rshCD6 no longer appears to provide an advantage.

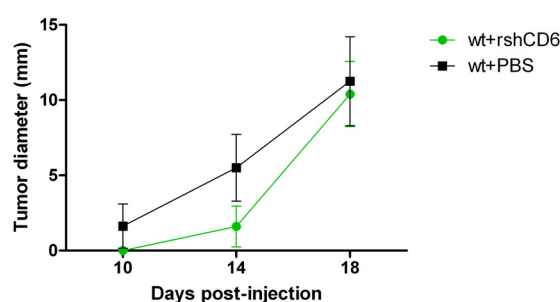


Fig. 3.30 – Effect of rshCD6 as a chemotherapy adjuvant. 1×10^5 B16 cells were s.c. inoculated into two groups of C57BL/6 WT mice ($n=5$). One group received a $25 \mu\text{g}$ rshCD6 treatment (green) and the other the same volume of PBS (black). Three days post-tumor inoculation, both groups received a single dose of chemotherapy (Vincristine 1 mg/kg and Doxorubicin 3.3 mg/kg). The tumor was measured with a caliper. Data are presented as mean \pm SD.

4. Discussion

As previously mentioned, this work had as main objective the study of two proteins belonging to the SRCR-SF sharing high homology with each other: CD5 and CD6. No unifying function for the members of this superfamily has been described, but it has been reported that some of them bind to and recognize PAMPs. The importance of studying these two molecules resides in the fact that they possess immunomodulatory functions; however, the exact nature of these properties warrants further study. For example, evidences demonstrate that CD5 negatively modulates the immune response, particularly in the cells where it is expressed, T and B cells (Soldevila, 2011); however, the ligand of CD5, a very controversial topic, remains to be found. The ligand of CD6, ALCAM, has been identified, but the relevance of this interaction to the immune response remains to be explained in full. Due to its presence at the immune synapse and high homology with CD5, it may be considered that this molecule also plays a role on the modulation of lymphocyte response.

Thus, this work attempted to answer several questions about CD5 and CD6 in order to further the knowledge on these proteins and their importance to the immune response.

4.1. Functional study of rshCD5 in the homeostasis of regulatory and effector lymphocyte subpopulations

As already mentioned, the rshCD5Tg mice developed in this laboratory present an exacerbated immune response observed through the induction of experimental autoimmune diseases and explained by a decrease in regulatory subpopulations. rshCD5Tg mice were found to express an average of 5 to 8 ng per mL of rshCD5 in serum, which had the same characteristics and biochemical properties as those described before for this molecule (Calvo *et al.*, 1999). These mice were routinely tested by PCR for expression of the transgene, and rshCD5 was detected in their serum by immunoprecipitation. After confirmation of rshCD5 expression, several tests involving analysis of subpopulations of the immune system were carried out to further characterize the rshCD5Tg mice model. The results were confirmed by injecting rshCD5 to C57BL/6 WT mice, in order to ascribe without doubt the phenotype of transgenic mice to the presence of rshCD5. It should be noted that the rshCD5 injected was also tested to verify that its biochemical properties were appropriate and that the molecule was functional.

There are two basic distinct subpopulations of T lymphocytes defined by their expression of $\alpha\beta$ TCR or $\gamma\delta$ TCR. They arise from a common precursor, the double negative (DN) thymocytes, but unlike the $\alpha\beta$ T cells which are found mostly in the thymus and lymph nodes, the $\gamma\delta$ T cells are normally in the epithelium and mucosa-associated lymphoid tissues where they maintain the integrity of the epidermis and regulate the homeostasis of intestinal epithelium (Ciofani and Zúñiga-Pflücker, 2010). Clearance of viruses and bacteria have also been ascribed as functions of these cells, and it has

also been reported that they can eliminate parasites. The peripheral $\gamma\delta$ T cells can also exert several regulatory and effector functions contributing to immune suppression (Hao *et al.*, 2010). Furthermore, it has been reported that murine Treg cells can abolish key effector functions and proliferation of the $\gamma\delta$ T lymphocytes *in vivo* and *in vitro*, and that this suppression is dependent on direct contact between these cell types (Hao *et al.*, 2010).

As previously mentioned, CD5 is a molecule considered to be a bridge between the innate and the adaptive immune system, with roles in modulating lymphocyte activation, fungi aggregation, etc. The $\gamma\delta$ T cells also constitute a bridge between both types of immune response, since they can recognize specific Ag without MHC restriction. This common feature (sharing functions involved in both the innate and the adaptive immune response) led to the hypothesis that the presence of rshCD5 in serum could interfere with the homeostasis/dynamics of $\gamma\delta$ T cells. When the percentage of this population was analyzed by flow cytometry in rshCD5Tg and non-Tg mice, it was found that these cells were expanded in transgenic mice. This observation is in agreement with previous results obtained in this mouse model, since the Treg cell population is reduced in rshCD5Tg mice, and in this way the $\gamma\delta$ T cells could expand. These results are also in agreement with tumor experiments due to the involvement of $\gamma\delta$ T cells in the antitumor response (see section 4.3.).

Another subpopulation analyzed by flow cytometry was that constituted by marginal zone B cells. Despite the fact that expression of CD5 has not yet been described in these cells (Bendelac *et al.*, 2001), it is known that they share phenotypic and/or functional characteristics with the B1-a cells, which express high levels of CD5. In rodents, the MZ B cell population resides in the outer white pulp of the spleen and expresses high levels of CD1d and CD21 that facilitate the transport of immune complexes from the circulation to the spleen, where they are subsequently presented to follicular B lymphocytes. Thus, it is said that these cells are important in the late phases of infection, when pathogens are in the blood and are filtered in the marginal zone of the spleen. The MZ B cells are also part of the “natural immune memory” and contribute to T cell independent type 2 immune responses. However, B1 cells are also needed for an adequate response, since these cells are important to halt early bacterial growth at the site of infection. These two populations, MZ and B1 cells, are involved in the production of IgM, an immunoglobulin that recognizes repetitive polysaccharide Ag (a type of Ag which generates a T cell-independent type 2 response) (Pillai and Cariappa, 2009; Wardemann *et al.*, 2002). Moreover, MZ B cells share some phenotypic and functional characteristics with the B1-a cells (Martin *et al.*, 2001), and even some similarities with the regulatory B cells (CD1d^{high}CD21^{high}).

When MZ cells were analyzed in rshCD5Tg mice, it was shown that transgenic mice possess a higher proportion of these cells than their non-transgenic littermates. As previously mentioned, these cells are excellent Ag-presenting cells, and probably are involved in the early events of the T cell-independent and also T-cell dependent immune responses (see section 4.2.). The observed increased in

this subpopulation is then consistent with the enhanced immune response displayed by rshCD5Tg mice.

The last subpopulation studied was the NKT cells, which co-express phenotypic markers of T and NK cells (Matsuda *et al.*, 2008). NKT cells are true T cells, derive from conventional T lymphocytes, and not NK cells; they possess a true TCR and CD3 complex, but also have some innate immunity functions and express NK1.1, marker of NK cells (Berzofsky and Terabe, 2008).

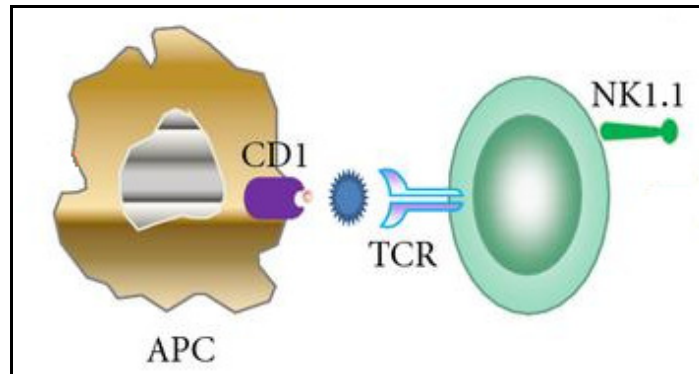


Fig. 4.1. – NKT cells express the surface marker NK1.1 and a semi-invariant T cell receptor (TCR). The antigen-presentation is carried out by CD1⁺ antigen presenting cells (APCs). CD1 molecules present lipid antigens to NKT cells. Upon ligation of CD1 via TCR, naïve NKT cells are activated, and respond rapidly to secrete high levels of cytokines, which play a critical role in the modulation of immune and inflammatory responses. Adapted from Zhang *et al.*, 2010.

These cells recognize non-protein Ag (such as glyco-lipidic Ag) through their $\alpha\beta$ TCR presented by non-classic MHC class I cells, such as CD1d⁺ cells. This subpopulation is also considered as a bridge between innate and adaptive immunity, since NKT cells quickly respond to TCR stimulation by releasing cytokines and chemokines, but also have the capacity to kill other cells, participate in bacterial clearance, regulate humoral response and contribute to Ab-specific-Ag responses (Matsuda *et al.*, 2008). NKT cells thus play an important role in modulating the immune response against tumors, infections and autoimmune disorders. These cells also express CD5 (Arrunategui-Correa *et al.*, 2004), so it would be expected that their dynamics and homeostasis in rshCD5Tg mice might be affected.

There was a tendency for NKT cells to be increased in rshCD5Tg mice, but the low number of mice and the intrinsic variability of each mouse might account for the result not being statistically significant (already observed in Fenutria, 2011). This tendency for an increase in NKT cells could be explained by two hypotheses; on the one hand, this subpopulation has been reported to synergize with the $\gamma\delta$ T lymphocytes (Matsuda *et al.*, 2008), themselves increased in this model. On the other hand, it is known that Treg cells can suppress the function of NKT cells by cell-contact-dependent mechanisms (Matsuda *et al.*, 2008); since Treg cells are decreased in rshCD5Tg mice, this might account for an increase in NKT cell proliferation, in a similar way to $\gamma\delta$ T cells.

To confirm that the results were not due to the effects of random insertion of the transgene, C57Bl/6 WT mice were treated with rshCD5 for 15 days every 48 hours. It must be taken into account that this experiment was carried out with a very small number of mice (n=3) and the variability of the cell numbers must be taken into account. In this assay several lymphocyte subpopulations were studied, and in general the results obtained with rshCD5Tg mice were reproduced: an increased percentage of NK and NKT cells and a decreased percentage of Treg cells were observed. It should be noted that NK cells represent the arm of the innate immune system, as opposed to NKT cells, which act as a bridge between the innate and adaptive response, participating in the early defense against intracellular microbial infections, immunosurveillance and autoimmune/hypersensitivity reactions (Bryceson *et al.*, 2011).

In addition to rshCD5, C57Bl/6 WT mice were also treated with rshCD6 on comparable schedules. The effects of prolonged injection of rshCD6 had never been studied, but since these two molecules are highly homologous it would be expected that their modulation of lymphocyte populations might be similar. Unexpectedly, it was found that treatment with rshCD6 had the opposite results to treatment with rshCD5: the percentage of NKT cells was lower and the proportion of Treg cells was higher. However, the percentage of B1-a cells was decreased as compared to mice treated with PBS, in a similar way to what happened to C57Bl/6 WT mice treated with rshCD5. A recent review suggests that regulatory B cells are at the center of the immune response, and thus changes in this subpopulation might then be responsible for the induction of changes in other subpopulations (Mauri, 2010). In this way, a change in B cells with regulatory function might be enough to cause alterations in other cell types, such as NKT and Treg cells; since prolonged administration of both rshCD5 and rshCD6 appear to induce the same decrease in B cells with regulatory function, this might suggest that both molecules may induce a similar effect. However, this must yet be confirmed.

Altogether, the results from the further characterization of immune cell subpopulations in rshCD5Tg mice are in agreement with previous observations and with the phenotype displayed by these mice, particularly the enhanced immune response shown by experimentally induced autoimmune disease. The role of CD5 and CD6 as immunomodulators appears to affect a number of different cell types, especially those that, like CD5 and CD6 themselves, are part of both the innate and adaptive immune response. However, some of the results obtained here were unexpected and further studies must be carried out in order to confirm whether they are reproducible or not.

4.2. Study of the rshCD5Tg mice immune response to TD and TI antigens

As aforementioned, the rshCD5Tg mice presented an exacerbated immune response in models of experimental autoimmune diseases. To better understand the mechanism/s behind this behavior, the Ag T cell-dependent (TD) and T cell-independent (TI) type 1 and 2 response was studied.

rshCD5Tg mice exhibit a more pronounced Ag TD response as compared to non-Tg mice. It is likely that this differential response could be due to changes in the T/B regulatory populations, which downregulate the immune response and which are decreased in the rshCD5Tg mice. Treg cells have specifically been described to control the immune response to TD Ag (Shan *et al.*, 2011 and Paust *et al.*, 2011). As previously shown, B regulatory cells are also decreased in these mice, but their importance is greater in the TI Ag response, as will be shown later.

Two types of TI Ag response were analyzed, type 1 (against LPS) and type 2 (against Ficoll). The results obtained were interesting in that it was found that in rshCD5Tg mice the Ab-specific-Ag type 1 response was exacerbated but not that of type 2. Once again it is likely that the type 1 response is more affected by the alteration of the homeostasis of regulatory and effector subpopulations; in other words, in basal conditions the CD5⁺ B cells (B1-a), and especially the subpopulation of regulatory B10 cells, are diminished. This decline *per se* could justify an increased response to TI antigens. However, it is noteworthy that rshCD5Tg mice exhibit a concomitant increase in the marginal zone B cell subpopulation (MZ B). This subpopulation is involved primarily in the response to TI-2 antigens, although it is known that MZ B cells actively proliferate and differentiate into plasma cells in response to low doses of TI-1 Ag (LPS), even before than follicular B cells or B2 cells (Martin and Kearney, 2000). In the immune response against bacterial antigens associated with TI Ag, the first wave of plasma cells clearly derived from B cells exhibit a phenotype similar to that of MZ and B1 cells. Based on this information, it is difficult to understand the lack of a TI-2 exacerbated response in rshCD5Tg mice. This could be explained by a compensation mechanism in response to the decrease in B1-a cells and the increase in MZ B cells, but this warrants further study, especially to improve the existing knowledge on the similarities and differences between MZ B cells and B1 cells, and whether they have complementary or redundant functions.

The observed exacerbation in antibody responses against TD and TI antigens in rshCD5Tg mice suggests that there could be a use for rshCD5 as an adjuvant in future vaccine strategies against TD or TI-1 antigens.

4.3. Tumor models in rshCD5Tg mice

Our findings showed that rshCD5Tg mice displayed an exacerbated response in experimental autoimmune models and in Ag TD and TI responses, so it was considered of interest to study the other side of the immune response, the anti-tumor response in murine models of cancer (Dalloul, 2008). In other words, the mechanisms that increase the susceptibility to autoimmune processes are also the mechanisms underlying the antitumor response. In the transgenic model studied in this work, the reduction of regulatory T and B subpopulations increased the severity of experimentally-induced autoimmune processes (Fenutría, 2011), something that might also increase the effectiveness and "strength" of the antitumor response (Yamazaki *et al.*, 2011). Thus, to study this process, we

analyzed four widely used mouse models of cancer: melanoma, sarcoma, lymphoma and colon carcinogenesis.

The B16 is a well-established mouse melanoma cell line used in the study of experimental cancer, which was originated in the syngeneic C57BL/6 (H-2b) mouse strain. B16 cell growth in rshCD5Tg mice was found to be slower than in non-Tg mice. This observation could be explained by changes in the homeostasis of regulatory T and B lymphocytes (lower proportion, so less suppression of the response) as well as of cytotoxic effector NK, NKT and $\gamma\delta$ T cells (higher proportion, so stronger response) that form the basis of anti-tumor response. The aforementioned effector cytotoxic subpopulations are involved in the antitumor immune response, and it has reported that these cells can specifically lyse and suppress the growth of various tumor cell lines (Hao *et al.*, 2010). Other, yet unknown, direct effects of circulating rshCD5 may also be responsible for the slower tumor growth in rshCD5Tg mice. In the chemotherapy assays, it was found that the administration of rshCD5 and rshCD6 as adjuvants for chemotherapy also decreased tumor growth compared to those mice treated with chemotherapy and PBS. Although preliminary results with prolonged administration of rshCD6 have shown different changes in cell subpopulations from those caused by prolonged administration of rshCD5, it would seem that somehow both molecules synergize similarly with chemotherapy in the antitumor response. This effect may be due to the prolonged administration of these molecules leading to alterations in lymphocyte population homeostasis that are functionally relevant to this response. Moreover, chemotherapy itself influences the antitumor response, since the lysis of tumor cells releases more antigens to be presented to immune cells and activate them; rshCD5 and rshCD6 might then enhance this response. As mentioned in section 4.1, a change in B cells with regulatory function, which appears to be caused by prolonged administration of both rshCD5 and rshCD6, might be enough to induce changes in other subpopulations and alter the antitumor response; this could explain the similar effect both molecules have in the chemotherapy treatment of B16 melanoma tumors. If confirmed, these results would put B cells with regulatory functions at the center of the anti-tumor response, with a much more important role than was previously ascribed to them.

Similar results, albeit less dramatic, were observed in the other two models studied, the MCA 205 fibrosarcoma cell line and the RMA-S T-cell lymphoma cell line, although it is necessary to optimize the amount of cells to be injected. These models involve cells which are less immunogenic than the B16 cells, but it is still possible to see a discrete improvement in the antitumor response of rshCD5Tg mice compared to non-Tg mice. It should be noted that these two models were carried out to verify that the response observed was not specific for melanoma, but it also applies to other tumors with different features. A preliminary study of cytokine levels present in MCA 205 tumors was carried out and its results reinforce the idea that the tumor environment is less immunosuppressive (lower IL-10 levels and higher IL-6 levels) in rshCD5Tg mice than in non-Tg mice.

The last studied model was the AOM/DSS murine model of colon carcinogenesis. This is a model of cancer of inflammatory origin that leads to the appearance of tumors in the colon. The

preliminary results show that rshCD5Tg mice display a lower number of tumors in both colon and small intestine. However, the assay should be repeated with a larger number of mice in order to confirm these results. Altogether, these results show that the presence of rshCD5, and also rshCD6, is able to modulate the anti-tumor response, presumably through the induced changes in lymphocyte subpopulation dynamics. These results also show a beneficial effect of rshCD5, and also of rshCD6, for the treatment of experimentally induced tumors in mice.

4.4 Conclusions and future perspectives to further this study

The results presented here support the therapeutic potential of the administration of soluble forms of rshCD5 and rshCD6 in different clinical situations of interest such as tumors, septic shock (of fungal origin for rshCD5 and of bacterial origin for rshCD6), as well as vaccine interventions against antigens which are poorly immunogenic or in patients with depressed immune systems (such as those undergoing immunosuppressive therapies and those suffering from congenital immunodeficiencies).

Prolonged administration of these molecules induces changes in lymphocyte subpopulations that may enhance the anti-tumor response, as demonstrated by the results in murine cancer models, but also induce exacerbated immune responses against exogenous Ag such as infectious microorganisms. Thus, chronic administration of rshCD5 and rshCD6 could be beneficial in situations of chronic infection in which the immune system is unable to respond effectively for the complete elimination of the infection.

Here again it was possible to verify that CD5 and CD6 have immunomodulatory properties, but further studies must be conducted to answer questions raised in part by this work and that remained unanswered. It would be interesting to continue the assays of murine tumor models already begun in order to optimize them and to perform them with a higher number of animals. Moreover, Tumor-Infiltrating-Lymphocytes will be interesting to analyze; the number of infiltrating cells, as well as which cell populations are present and the nature of the intratumor cytokine patterns are all worthy of study. It would also be interesting to analyze the functionality of the Treg cells, to find out whether the observed differences in the rshCD5Tg mice are only at the level of numbers or whether the function of these cells is also affected.

Much less is known about the role of CD6 in the immune system, but this group will soon have at its disposal CD6 knockout mice which will make possible the in-depth analysis of the role of CD6 in immune system development and response.

5. References

Abbas, A. K., Lichtman, A. H., Pillai, S. 2007. Cellular and Molecular Immunology. Philadelphia: Saunders Elsevier. 6th edition.

Alberola-Illa, J., Places, L., Cantrell, D. A., Vives, J., Lozano, F., 1992. Intracellular events involved in CD5-induced human T cell activation and proliferation. *Journal Immunology* 148(5):1287-1293.

Arman, M. 2004. Regulació transcripcional de les proteïnes limfocítiques CD5 i CD6. Doctoral Thesis. Health Sciences Division, Department of Cell Biology and Pathological Anatomy, Faculty of Medicine, University of Barcelona

Arrunategui-Correa, V., Lenz, L., Kim, H. S. 2004. CD1d-independent regulation of NKT cell migration and cytokine production upon *Listeria monocytogenes* infection. *Cell Immunology* 232(1-2):38-48.

Aruffo, A., Bowen, M. A., Patel, D. D., Haynes, B. F., Starling, G. C., Gebe, J. A., Bajorath, J. CD6-ligand interactions: a paradigm for SRCR domain function. *Immunology Today* 18(10):498-504.

Baumgarth, N. 2011. The double life of a B-1 cell: self-reactivity selects for protective effector functions. *Nature Reviews Immunology* 11:34-46.

Bendelac, A., Bonneville, M., Kearney, J. F. 2001. Autoreactivity by design: innate B and T lymphocytes. *Nature Review Immunology* 1(3):177-186.

Berzofsky, J. A., Terabe, M. 2007. A novel immunoregulatory axis of NKT cell subsets regulating tumor immunity. *Cancer Immunology Immunotherapy* 57(11):1679-1683.

Bikah, G., Carey, J., Ciallella, J. R., Tarakhovsky, A., Bondada, S. 1996. CD5-mediated negative regulation of antigen receptor-induced growth signals in B-1 B cells. *Science* 274(5294):1906-1909.

Bowen, M. A., Aruffo, A. A., Bajorath, J. 2000. Cell Surface Receptors and Their Ligands: In Vitro Analysis of CD6-CD166 Interactions. *Proteins: Structure, Function and Genetics* 40:420-428.

Brown, M. H., Lacey, E. 2010. A ligand for CD5 is CD5. *Journal of Immunology* 185:6068-6074.

Bryceson, Y. T., Chiang, S. C. C., Darmanin, S., Fauriat, C., Schlums, H., Theorell, J., Wood, S., M. 2011. Molecular Mechanisms of Natural Killer Cell Activation. *Journal of Innate Immunity* 3:216–226.

Calvo, J., Places, L., Padilla, O., Vila, J. M., Vives, J., Bowen, M. A., Lozano, F. 1999. Interaction of recombinant and natural soluble CD5 forms with an alternative cell surface ligand. *European Journal of Immunology* 29:2119-2129.

Ciofani, M., Zúñiga-Pflücker, J. C. 2010. Determining $\gamma\delta$ versus $\alpha\beta$ T cell development. *Nature Reviews Immunology* 10(9):657-663.

Dalloul, A. 2008. CD5: a safeguard against autoimmunity and a shield for cancer cells. *Autoimmunity Reviews* 8:349-353.

Fenutría, R. 2011. Propiedades Inmunomoduladoras de la Región Extracelular de CD5. Doctoral Thesis. Immunology Unit, Department of Cell Biology, Immunology and Neuroscience, Faculty of Medicine, University of Barcelona

Goris, R. J., Boekholtz, W. K., Bebbber, I. P. van, Nuytinck, J. K., Schillings, P. H. 1986. Multiple-organ failure and sepsis without bacteria. An experimental model. *Archives of Surgery* 121(8):897-901.

Hao, J., Wu, X., Xia, S., Li, Z., Wen, T., Zhao, N., Wu, Z., Wang, P., Zhao, L., Yin, Z. 2010. Current progress in $\gamma\delta$ T-cell biology. *Cellular & Molecular Immunology* 7(6):409-413.

Janeway, C.A. Jr., Travers, P., Walport, M., *et al.* 2001. *Immunobiology: The Immune System in Health and Disease*. New York: Garland Science. 5th edition.

Lozano, F., Simarro, M., Calvo, J., Vila, J. M., Padilla, O., Bowen, M. A., Campbell, K. S. 2000. CD5 signal transduction: positive or negative modulation of antigen receptor signaling. *Critical Review Immunology* 20(4):347-358.

Martin, F., Kearney, J. F. 2000. B-cell subsets and the mature preimmune repertoire. Marginal zone and B1 B cells as part of a "natural immune memory". *Immunology Review* 175:70-79.

Martin, F., Oliver, A. M., Kearney, J. F. 2001. Marginal zone and B1 B cells unite in the early response against T-independent blood-borne particulate antigens. *Immunity* 14(5):617-629.

Mataalka, K. Z., Tutunji, M. F., Abu-Baker, M., Baker, Y. A. 2005. Measurement of protein cytokines in tissue extracts by enzyme-linked immunosorbent assays: Application to lipopolysaccharide-induced differential milieu of cytokines. *Neuroendocrinology Letters* 26(3):231-236.

Matsuda, J. L., Mallevaey, T., Scott-Browne, J., Gapin, L. 2008. Cd1d-restricted iNKT cells, the "Swiss-Army knife" of the immune system. *Current Opinion on Immunology* 20(3):358-368.

Mauri, C. 2010. Regulation of immunity and autoimmunity by B cells. *Current Opinion in Immunology* 22(6):761-767.

Paust, H. J., Ostmann, A., Erhardt, A., Turner, J. E., Velden, J., Mittrucker, H. W., Sparwasser, T., Panzer, U., Tiegs, G. 2011. Regulatory T cells control the Th1 immune response in murine crescentic glomerulonephritis. *Kidney Int.* 80(2):154-64.

Pena-Rossi, C., Zuckerman, L. A., Strong, J., Kwan, J., Ferris, W., Chan, S., Tarakhovsky, A., Beyers, A. D., Killeen, N. 1999. Negative regulation of CD4 lineage development and responses by CD5. *Journal Immunology* 163(12):6494-6501.

Pillai, S., Cariappa, A. 2009. The follicular versus marginal zone B lymphocyte cell fate decision. *Nature Reviews Immunology* 9(11):767-777.

Sarrias, M. R., Gronlund, J., Padilla, O., Madsen, J., Holmskov, U., Lozano, F. 2004. The Scavenger Receptor Cystein-Rich (SRCR) Domain: An ancient and highly conserved protein module of the innate immune system. *Critical Reviews in Immunology* 24(1):1-38.

Sarrias, M. R., Farnós, M., Mota, R., Sánchez-Barbero, F., Ibáñez, A., Gimferrer, I., Vera, J., Fenutría, R., Casals, C., Yélamos, J., Lozano, F. 2007. CD6 binds to pathogen-associated molecular patterns and protects from LPS-induced septic shock. *PNAS* 104 (28): 11724-11729.

Sellick, G. S., Wade, R., Richards, S., Oscier, D. G., Catovsky, D., Houlston, R. S. 2008. Scan of 977 nonsynonymous SNPs in CLL4 trial patients for the identification of genetic variants influencing prognosis. *Blood* 111:1625-1633.

Shan, J., Guo, Y., Luo, L., Lu, J., Li, C., Zhang, C., Huang, Y., Feng, L., Wu, W., Long, D., Li, S., Li, Y. 2011. Do CD4(+)Foxp3(+) Treg cells correlate with transplant outcomes: A systematic review on recipients of solid organ transplantation. *Cell Immunology* 270(1):5-12.

Smith-Garvin, J. E., Koretzky, G. A., Jordan, M. S. 2009. T cell activation. *Annual Review Immunology* 27:591-619.

Soldevila, G., Raman, C., Lozano, F., 2011. The immunomodulatory properties of the CD5 lymphocyte receptor in health and disease. *Current Opinion Immunology* 23(3):310-318.

Stamou, P., Jersey, J., Carmignac, D., Mamalaki, C., Kioussis, D., Stockinger, B. 2003. Chronic exposure to low levels of antigen in the periphery causes reversible functional impairment correlating with changes in CD5 levels in monoclonal CD8 T cells. *Journal Immunology* 171(3):1278-1284.

Suzuki, R., Hiroyuki, K., Sugie, S., Nakagama, H., Tanaka, T. 2006. Strain differences in the susceptibility to azoxymethane and dextran sodium sulfate-induced colon carcinogenesis in mice. *Carcinogenesis* 27(1):162-169.

Velde, H. V. d., Hoegen, I. v., Luo, W., Parnes, J. R., Thielemans, K. 1991. The B-cell surface protein CD72/Lyb-2 is the ligand for CD5. *Nature* 351(6328):662-665.

Vera, J., Fenutría, R., Cañadas, O., Figueras, M., Mota, R., Sarrias, R-M., Williams, D. L., Casals, C., Yelamos, J., Lozano, F. 2009. The CD5 ectodomain interacts with conserved fungal cell wall components and protects from zymosan-induced septic shock-like syndrome. *PNAS* 106(5):1506-1511.

Verwilghen, J., Vanderberghe, P., Wallays, G., Boer, M. d., Anthony, N., Panayi, G. S., Ceuppens, J. L. 1993. Simultaneous ligation of CD5 and CD28 on resting T lymphocytes induces T cell activation in the absence of T cell receptor/CD3 occupancy. *Journal Immunology* 150(3):835-846.

Wardemann, H., Boehm, T., Dear, N., Carsetti, R. 2002. B-1a B cells that link the innate and adaptive immune responses are lacking in the absence of the spleen. *J Exp Med.* 195(6):771-80.

Yamazaki, S., Okada, K., Maruyama, A., Matsumoto, M., Yagita, H., Seya, T. 2011. TLR2-Dependent Induction of IL-10 and Foxp3⁺ CD25⁺ CD4⁺ Regulatory T Cells Prevents Effective Anti-Tumor Immunity Induced by Pam2 Lipopeptides In Vivo. PLoS One 6(4):e18833.

Zhang, H., Wu, J., Zhu, J. 2010. The Role of apolipoprotein E in Guillain-Barré Syndrome and Experimental Autoimmune Neuritis. Journal of Biomedicine and Biotechnology 2010:357412.